The University of South Bohemia in České Budějovice
Faculty of Science

Characterization of *Bartonella* species infecting North American Triatominae (kissing bugs)

Bachelor thesis

Alexandra Kogler

Advisor: Eva Nováková, PhD.

České Budějovice 2021

Kogler A., 2021: "Characterization of *Bartonella* infecting North American Triatominae (kissing bugs)", Bc. Of Science Thesis in English, 47 p. Faculty of Science, University of South Bohemia, České Budějovice, Czech Republic.

Annotation

The aim of this thesis was to characterize *Bartonella* spp. within *T. rubida* gut microbiomes, using multilocus sequence typing (MLST), and to determine its incidence at different sampling localities.

Declaration

I hereby declare that I have worked on my bachelor's thesis independently and used only the sources listed in the bibliography.

I hereby declare that, in accordance with Article 47b of Act No. 111/1998 in the valid wording, I agree with the publication of my bachelor thesis, in full to be kept in the Faculty of Science archive, in electronic form in publicly accessible part of the STAG database operated by the University of South Bohemia in České Budějovice accessible through its web pages. Further, I agree to the electronic publication of the comments of my supervisor and thesis opponents and the record of the proceedings and results of the thesis defence in accordance with aforementioned Act No. 111/1998. I also agree to the comparison of the text of my thesis with the Theses.cz thesis database operated by the National Registry of University Theses and a plagiarism detection system.

15.8.2021, Linz

Signature .....

Alexandra Kogler

Acknowledgements

I would like to thank my Supervisor Eva for her help during the writing process and throughout all difficulties that appeared. She always gave her best to support me in the last few months and I am grateful to have had such a patient supervisor like her. Working in this Institute was such a great experience, and I can really recommend working there. I also want to thank my Co-Supervisor Giampiero Batani (PhD) for the help in the laboratory.

Abstract

Triatominae are vectors of medically highly relevant pathogen, *Trypanosoma cruzi*, and lately they have become a great health concern in the United States. There are over 150 species of Triatominae known. While the majority distributes over Central and South America, there are 11 native species found in the US.

In this study, the focus lies on *Triatoma rubida,* one of the broadly distributed species that can invade human domiciles, and its association with bacteria of the genus *Bartonella*.

T. rubida samples were collected from nests of the white-throated packrat in two different habitats in Arizona. MLST four housekeeping genes (16S rRNA, gltA, rpoB and groEL) was performed to characterize *Bartonella* spp. within *T. rubida* gut microbiomes.

The results of MLST were compared to high throughput amplicon data for 16S rRNA gene generated for some samples in 2018.

By comparing these results, it was illustrated that the location, ontogeny, and year of collection play a key role in *Bartonella* determination. The highest *Bartonella* incidence, by looking at the location and year of sampling, was given by the samples collected in Las Cienegas National Conservation Area (LC) in 2019. Besides that, it is demonstrated that the broadest diversity of Bartonella species were detected by 16S rRNA, but for the phylogenetic analysis no reasonable result was obtained. By comparing the phylogenetic trees of the different housekeeping genes, it can be detected that gltA performed best for this sample set.

Content of the thesis

1. Introduction

1.1 Triatominae as vectors of disease

Triatominae, also known as kissing bugs, are hemimetabolous blood-feeding insects that undergo five larval stages before they reach adulthood. There are more than 150 Triatominae species known which differ in distribution, biology and vectorial capacity. The majority of the species are found in Central and South America (Galvão *et al*., 2003; Brown et al., 2020; Rodríguez-Ruano et al., 2018), but there are 11 species native to the United States. North American kissing bugs are divided into two genera, *Triatoma* and *Paratriatoma* (Klotz et al., 2014). These species are either specializing in feeding on lizards, birds or mammals. (Klotz et al., 2014) In both Americas, Triatominae are a great public concern as they are vectors of Chagas disease, which is a life-threatening disease caused by an unicellular eukaryote, *Trypanosoma cruzi*. Since the infection rate and autochthonous Chagas disease cases in the United States have been increasing in recent years (Vieira et al., 2018; Bonney, 2014), North American Triatomines became an important research topic (Brown et al*.,* 2020). Generally, *T. cruzi* is disseminated by vector-borne transmission but Chagas disease can also be acquired by blood transfusion, ingestion of a contaminated bug or organ transplantation (Klotz et al., 2014*).*

Furthermore, other parasites, such as *T. rangeli.* can be propagated from Triatomine vectors. *Trypanosoma rangeli* is known to infect several domestic and wild animals in Latin America. In diagnostic and prophylactic aspects, the infection of *T. rangeli* is similar to Chagas disease. Generally, rodents and primates are the vertebrate natural reservoirs of *T. rangeli* (Bayão et al., 2020). *T. rangeli* is not pathogenic for vertebrates but for the vector. Furthermore, *T. cruzi* presents in the intestine of a Triatomine suggests a high risk of transmission, whereas finding *T. rangeli* is not an indication for the insect as a vector (Vallejo et al., 2009).

Kissing bugs normally occupy a variety of environments, such as grasslands, deserts, tropical forests, and urban areas (Gürtler et al*.,* 2007), where they live in nests and burrows of different mammals or humans' domiciles (Lazzari et al., 2013).

Due to their broad ecological niche, kissing bugs transmit Chagas disease in both, domestic and sylvatic disease cycles. The sylvatic cycle is between *Triatoma* species and wild animals while the domestic cycle covers the infected *Triatoma* species infesting humans' domiciles or domesticated animals (Gürtler et al., 2007; Cohen & Gürtler, 2001).

The eleven species of Triatominae which are considered to be native to North America are *T. gerstaeckeri, T. indictiva, T. recurva, T. rubida, T. incrassata, T. lecticularia, T. protracta, T. sanguisuga, T. rubrofasciata, T. neotomae* and *Paratriatoma hirsuta* (Bern et al., 2011). Each of the 11 species is a potential vector, but not all are frequently connecting the sylvatic and domestic cycle infesting humans' domiciles. Species that frequently connect the two cycles are *T. recurva, T. rubida* and *T. lecticularia* (Bern et al., 2011).

Mainly all infections within the Triatominae species are due to their blood-feeding behaviour (Vieira et al., 2018). *T. cruzi* enters the gastrointestinal tract while the Triatominae bug is sucking the blood of an infected host. The epimastigotes from the small intestine are then passed on to the rectum. In the terminal part of the abdomen, the infectious trypomastigotes line the rectal gland (Klotz et al., 2014). *Trypanosoma cruzi* is then excreted with the faeces and transmitted as the faeces contaminates the wound from which the kissing bug fed. Initially, human immune system reacts in swelling, anaphylaxis, severe fever and possible itching at the bite site (Klotz et al, 2010; Vieira et al., 2018).

There are two different phases of a *T. cruzi* infection, the acute and chronical phase. The acute phase occurs one to two weeks after infection, which is usually asymptomatic or very mild. Even though severe acute phase of Chagas disease is rare, the mortality risk is very high when it occurs (Bern et al., 2019). However, the chronic phase of an *T. cruzi* infection shows a damage of the heart muscle (Bern et al., 2019).

While humans are broadly secondary hosts (Mediannikov et al., 2013), the main reservoir for *T. cruzi* are wild and domesticated animals. Dogs and other domestic animals often get infected by the ingestion of a bug. While in South America wild pigs, wild goats and bats are implicated in spreading Chargas disease, in the USA, animals like opossums, armadillos and the packrats are accountable (Gürtler et al., 1993; Cohen & Gürtler, 2011).

One of the best-known Triatominae species associate with packrats in the Southern United States is the *Triatoma rubida* (Ribeiro et al., 2012). *T. rubida* is found in Arizona, California, Texas, New Mexico and various northern Mexican States (Pfeiler et al., 2006). The species belonging to the *rubrofasciata* complex (Ribeiro et al., 2012) is a potent vector of *T. cruzi* due to their defecation during feeding (Indacochea et al., 2017). Usually, *T. rubida* beset packrat (*Neotoma albigula*) nests or enter humans domiciles due to their attraction to light. *T. rubida* then feeds on humans, the pets in the household or the packrats nearby (Klotz et al., 2014).

Recently it has been shown that *T. cruzi* is not the only pathogen associated with *Triatoma* species. There is evidence that bacteria of the genus *Bartonella* are prevalent among all life stages of *T. rubida* and *T. protracta* individuals (Brown et al.,2020). Brown and colleagues described these bacteria as a generous element of *Triatoma* microbiome and suggested that *T. rubida* obtains *Bartonella* from the blood of its packrat hosts.

1.2 *Bartonella* species

Bartonellae are gram-negative, fastidious, curved vector-borne rod-shaped bacteria that infect the erythrocytes and endothelial cells of their hosts (Chomel & Kasten 2010). At the time the *Bartonella* species colonize the erythrocytes, they can infect the bloodstream with bacteraemia until the natural death of the cell occurs (Schulein R, et al., 2001). Generally, *Bartonella* species are known to be transmitted by blood-sucking arthropods (Eicher & Dehio, 2012), such as fleas, lies and ticks (Billeter et al., 2008).

Rodents are frequently involved in the transmission of this bacteria (Buffet et al., 2013) and are one of the natural reservoirs for a variety of *Bartonella* species (Gutiérrez et al., 2015)**.** Dogs, cats, foxes and deer are further possible animal hosts. Humans are normally secondary hosts, who got infected by accident (Mediannikov et al., 2013).

Within the 14 species of the genus *Bartonella (*Renesto et al*., 2001)*, at least seven rodent-borne *Bartonella* species or subspecies are recognized as human pathogens such as *Bartonella grahamii, Bartonella tribocorum, Bartonella elizabethae, Bartonella vinsonii* subsp*.auupensis, Bartonella vinsonii* subsp. *vinsonii Bartonella tamiae* and *Bartonella washoensis* (Buffet et al., 2013). Members of this genera are associated with several symptoms in humans, which include fever, endocarditis, lymphadenitis and myocarditis (Kaiser et al., 2011).

Most of the rodent species stay infected by these microorganisms for a long time, typically with different *Bartonella* variants, as they are able to replace one another (Paziewska et al., 2012). Diversification, which occurs by homologous recombination, is a common strategy for *Bartonella* species to rescue themselves from elimination by the host's immune system. However, this is just possible if the distances between the species are not increased (Fraser et al., 2007).

Concerning the efficiency of the transmission cycle for *Bartonella*, the rodent habitant may play a key role. In unfavourable conditions vectorial transmission of *Bartonella* does not occur. The geographic conditions and type of habitant can then lead to a higher vulnerability for bacterial infections (Gutiérrez et al., 2015**)**. In addition, physical contact, grooming and removal of the ectoparasites between the rodents can promote the transmission of *Bartonella* pathogens (Krasnov & Khokhlova, 2001). The parental behaviour of animals, such as licking or huddling, could also lead to an exposure of *Bartonellae*. Furthermore, the seasonality can affect the rate of rodent-rodent interactions and increase the risk of *Bartonella* infection (Krasnov et al., 2005). Nevertheless, these behaviours can be different among different rodent species (Gutiérrez et al., 2015).

1.3 Microbiomes of Triatominae

In general, blood-feeding insects are affected by their dedicated microbiomes (*Brown et al.,* 2020). For a better control strategy of Triatominae bugs, it is crucial to understand their gut microbiomes, as they influence their host traits. Microbiomes commonly influence the capacity of insect vectors to transmit parasites or pathogens (Rodríguez-Ruano et al., 2018). In addition, they also affect other fundamental aspects of their host biology, such as digestion, immunity and thermal tolerance (Brown et al., 2020). Furthermore, host fitness and a variety of phenotypic traits are defined by the insect microbiomes (Klepzig et al., 2009).

Symbiotic bacteria within the gut microbiomes are supposedly essential as they synthesise vitamins and simplify the blood meal digestion of their hosts (Brown et al., 2020). Unfortunately, there are only a few studies about Triatominae microbiomes having a lack of consistent patterns (Mann et al., 2020). This could be due to inconsistency between methodology or DNA templates that differ for most of the published work. On the other hand, it could also show the true biology of kissing bugs (Brown et al., 2020). Triatominae biological characteristics are very complex particularly due to the lengthy development in the five nymphal instars (Rodríguez-Ruano et al., 2018) and accessory feeding strategies like hemolymphorphagy, feeding on arthropod haemolymph, cleptohematophagy, known as feeding on the blood meal of another Triatomine bug (Durán et al., 2016) and coprophagy, where the Triatomine bugs consumes faeces of conspecifics (Díaz et al.,2016).

Furthermore, Brown et al. (2020) describes that the microbiomes of Triatominae have a significant loss in bacterial diversity throughout their development. In their study, it was shown that the first instars have the highest bacterial diversity, whereas the adult microbiomes are characterized by being dominated with a single bacterial taxon. For *T. rubida*, the genus *Dietzia* dominates the adult stage (Brown et al., 2020). Considering every life stage of *T. rubida*, *Bartonella* was the second most abundant taxa. In addition, Brown et al. (2020) indicates that the microbiomes are characterized based on their locality. Therefore, the microbiome variability differs in the nest origin, at least for early instars (L1-L3).

As the *Trypanosoma cruzi* undergoes its development through different types of mastigotes in the intestinal tract of the Triatominae species, it interacts with gut microbes. The interaction between *T. cruzi* and the microbiome can either be direct, through competition, or by indirect contacts, such as an increase of antiparasitic molecules or immunity modulation (Rodríguez-Ruano et al., 2018). Contrary, the life cycle of a related *Trypanosoma* species*, T. rangeli* does not allow for an extensive contact with the gut microbiome. Generally, *T. rangeli* leaves the gastrointestinal tract and relocates to the hemocoel. Then, it attacks the salivary glands, from where *T. rangeli* can be transmitted while feeding.

Contrary to eukaryotic pathogens, bacterial pathogens, like *Bartonella,* can establish much closer interaction with other bacterial members of the microbiome. Such interactions can be promoted through horizontal gene transfer (HGT). Generally, bacteria use HGT to adapt to unstable environments by acquiring new functions. HGT happens frequently among the gut bacteria and can be conserved within a single host individual, even though it is not clear if the gut microbiome is changed over an individual's lifetime (Groussin et al., 2021).
In addition, Groussin and colleagues. suggested that HGT in vertebrate gut microbiome might be linked to industrialization (Groussin et al., 2021). Another mechanism underlining direct interactions of bacteria with other cells involves type IV secretion systems (T4SS). T4SS enables bacteria to secrete macromolecules into other bacterial cells in the microbiome or possibly the cells of the host and other present eukoryotes, including *T.cruzi*. T4SS mediated horizontal transfer is a major contributor to bacterial evolutions, as pathogenic bacteria use it to survive inside a eukaryotic host and making their proliferation easier (Sgro et al., 2019). While both mechanisms can be utilized by *Bartonella* cells, it is not clear to what extent this pathogen competes or corporates with natural kissing bug microbiome.

Even though there are some studies about *Bartonella* in *Triatoma* bugs, there is not much information about *Bartonella* in *T. rubida*. Previous investigations revealed influences of factors on the Triatomine gut composition (Brown et al., 2020), but the phylogenetic diversity remains understudied.

To evaluate the phylogenetic diversity of *Bartonella* associates, tools such as multilocus sequence typing with different housekeeping genes as molecular markers are used.

1.4 Housekeeping genes as molecular markers

Housekeeping genes are essential for an organism to maintain its basal cellular functions. These genes need to operate under normal conditions, regardless of their developmental stage, tissue type, external signal or cell cycle state (Eisenberg & Levanon, 2013). Housekeeping genes are a matter of particular interest for internal controls or computational studies (Thellin et al., 1999). In addition, multilocus sequence typing schemes are based on housekeeping genes (Margos et al., 2008), as they are able to strain lineages, which are based on the short DNA sequences of these genes (Jans et al.,2016).

It is essential to compare different housekeeping genes to estimate their ability to delineate various species and subspecies. Even though 16S rRNA gene is the most conventional marker to define microbial ecology, it is known to be the one with the highest bias potential in amplicon sequencing (Ogier et al., 2019). Other taxonomic markers have been tested by targeting housekeeping genes (Poirier et al., 2018). To delineate different species of *Bartonella*, la Scola et al. (2003) compared some housekeeping genes, such as 16S rRNA, *gltA*, *groEL* and *rpoB*. The result of this experiment showed that *gltA* and *rpoB* were the most effective genes to distinguish between the species (La Scola et al., 2003). These housekeeping genes have all different functions. 16S rRNA is the coding gene for16S rRNA, *gltA* is the citrate synthase gene, *groEL* is the 60kDa heat-shock protein gene, *rpoB* is the RNA polymerase beta-subunit gene, *ribC* is essential for the riboflavin synthase and *ftsZ* is the cell division protein gene (Paziewska et al., 2011).

As a major tool for studying microbiome diversity, non-specific approach of 16S rRNA gene amplicon sequencing in a high throughput mode is used nowadays. This method development was driven forward by the human microbiome project (HMP) and the earth microbiome project. The HMP focussed on the gut investigating among other things on microbial communities and is a very large body-wide amplicon and metagenome survey.

By using shotgun sequencing, new aspects of microbiome have been characterized. Furthermore, new stain profiling techniques has distinguished subspecies population structures (Lloyd-Price et al., 2017). In the earth microbiome project amplicon sequencing in high throughput mode is used. This project focussed on interactions among microbes and their environment (Gilbert et al., 2010). In general, amplicon sequencing of 16S rRNA is verified to be an efficient and reliable approach to study microbiomes and taxonomic classification. 16S rRNA gene sequencing takes advantage of universal primers to amplify some of the nine regions (V1-V9), that are split by highly conserved sequences of the taxa. Therefore, the 16S rRNA gene sequencing is able to predict the functionality of the microbiota (Song & Xie, 2020). The bacterial identification is initiated by amplifying the gene with PCR with selected primers to anneal to the conserved regions. It is followed by high throughput sequencing to generate millions of amplicon reads that enable to distinguish between bacterial taxa in a microbiome (Matsuo et al., 2021).

2. Aim

The main focus in this research work will lie on *Triatoma rubida* and its association with the bacteria of the genus *Bartonella*. The goal of this study is to evaluate phylogenetic diversity of *Bartonella* associates and determine their prevalence in *T. rubida* samples originating from two different habitats in Arizona.

3. Materials and Methods

3.1 Sample collection and processing

A total of 154 *T. rubida* individuals were collected from nests of the white-throated packrat, *Neotoma albigula*, which were found at Las Cienegas National Conservation Area (LC) and the University of Arizona Desert Station (TU and DS). Both, of the localities offer the nests but differ in the proximity to human populated areas. While the University of Arizona Desert Station is bordering the city of Tucson with population of approximately 980 thousand people, Las Cienegas Conservation are is an area of 45000 acres with no permanent human population. Localities were sampled during 2018 (LC: n=45 and TU: n=78) and 2019 (DC: n=31) for all developmental stages, including five larval instars (L1-L5) and adults (designated as L6). Detailed information on the sample set is provided in *Table 10* in the appendix. For a better perception of the size of the larval instars and adult stages of kissing bugs, *Figure 1* was included. The samples were then preserved in vials with 100% ethanol and stored in -20°C before further analysis. Species molecular identification based on Cytochrome b (cytB) sequence was performed for all the analysed individuals by other lab members. Individuals determined as *T. rubida* were selected for the presented work based on the results of high throughput 16S rRNA amplicon analyses that revealed the highest abundance of *Bartonella* OUT in their microbiomes (read abundance provided by the supervisor presented in Table 11).

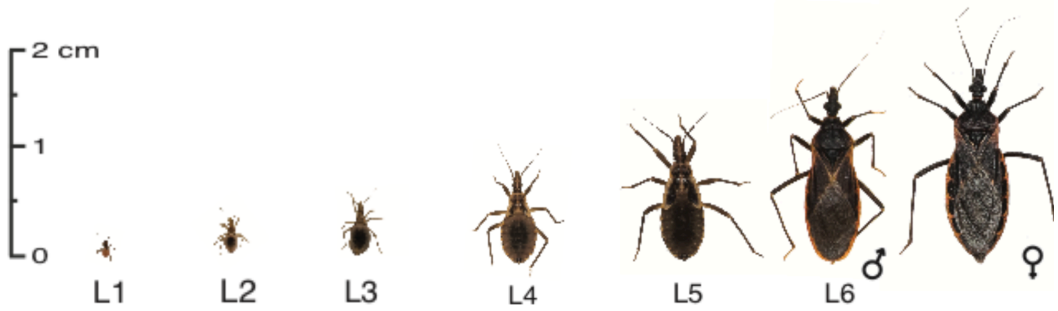

Figure 1: Ontogenetic stages of *Triatoma rubida* (Brown et al., 2020). Used with the authors permission.

3.2 DNA template of genomic DNA

Genomic DNA was isolated using QIAamp DNA Micro Kit (Qiagen, Hilden, Germany) from the whole abdomens. The isolation was performed according to the manufacturer's instructions by the other members of the research group. Thereby, the samples were prepared under the microscope, where they cut into pieces and washed with phosphate buffer solution. Next, the tissues were transferred into a tube and prepared for further washing steps and purification. The DNA was further on used as a template to identify the desired regions by Polymerase Chain Reaction (PCR).

3.3 Multilocus sequence typing (MLST)

Multilocus typing was performed for four housekeeping genes, 16S rRNA gene, gltA, rpoB and groEL. To prepare 25 µl of individual PCR reactions, 12.5 µl Combi PPP Master Mix (Top Bio, Vestec, Czech Republic) was mixed with 8.5 µl PCR Ultra H_2O (Top Bio, Vestec, Czech Republic), 1 µl for each of the primers (10 mol/L), and 2 µl of template DNA.

Amplification took place in a Master cycler (Eppendorf, Hamburg, Germany) with following conditions: 94°C for 2min followed by 40 cycles of 94°C for 45s, 60°C for 45s, 72°C for 45s, with a final extension of 72°C for 7min. Details on primers and conditions are given in *Table 2*. To verify the PCR products gel electrophoresis was carried out.

Table 1: Primer Sequences used for MLST analysis

Target Gene	Sequence (5'-3')	Length	Tm	Amplicon (bp)	Primer description	References
gltA	GGGGACCAGCTCATGGTGG	19	55	338	Forward	Norman et al., 1995; Paziewska et al., 2011
	AATGCAAAAAGAACAGTAAACA	22	55		Reverse	
rpoB	GCACGATTCGCATCATCATTTTCC	24	52	333	Forward	Renesto et al., 2001; Paziewska et al., 2011
	CGCATTATGGTCGTATTTGTCC	22	52		Reverse	
groEL	GAAGATGTGGAAGGTGAA	18	47	336	Forward	Renesto et al., 2001
	TCACGGTCATAGTCAGAAG	19	47		Reverse	
16S rRNA	TCAGAACGAACGCTGGCGGC	20	54	269	Forward	Paziewska et al., 2011
	CGTCATTATCTTCACCGG	18	54		Reverse	

3.4 Gel Electrophoresis

For the evaluation of the PCR products, a 1.5% agarose gel was prepared, and electrophoresis was carried out for all samples. For the gel, 80ml of TE buffer (ThermoFisher Scientific, Waltham, Massachusetts) was mixed with 1.2g agarose and 8µl GelRed Nucleic Acid Gel Stain. The TE buffer is important to solubilize the DNA and protect it from degradation. Gel red is an intercalating nucleic acid stain and used instead of ethidium bromide. 8 µl of the PCR product was pipetted into the prepared gel along with 1kb Ladder DNA (Gene Ruler 1kb, Thermo Scientific) added in the first well. For every gel a negative and positive control was added but 1 µl water was used instead of the DNA template. The gels were run for about 40-50 minutes at 120V. Gels containing separated DNA fragments were visualized under UV light using the UVITEC instrument.

3.5 Sanger Sequencing

PCR products were enzymatically purified using EXO 1 enzyme (Thermo Scientific, Waltham, Massachusetts) and Fast AP (Thermo Scientific, Waltham, Massachusetts) and Sanger sequenced in a single direction.

3.6 Phylogenetic analysis

The results of Sanger sequencing were analysed in the licenced software Geneious (http://www.geneious.com). First the sequences were cleaned from the primers and low-quality nucleotides were trimmed of. Using standard nucleotide BLAST (https://blast.ncbi.nlm.nih.gov/Blast.cgi) similar hits were retrieved from NCBI database. The matrices were compiled by multiple alignment of sequences using MUSCLE Alignment (Edgar 2004). PhyML program (Guindon et al., 2010) implemented in the ATGC-Montpellier platform (http://www.atgc-montpellier.fr) was used with Akaike information criterion (AIC) to select the best substitution model for each of the matrices (Smart Model Selection function). The phylogenetic trees were constructed for each matrix with Maximum Likelihood (ML) approach and bootstrap analyses were performed with 100 replicates using PhyML v. 3.0 (Guindon et al., 2010). Resulting trees were graphically visualized in Geneious (http://www.geneious.com). Inkscape (http://www.inkscape.org) was utilized for further graphical adjustments.

For 16S rRNA gene, *Brucella abortus* strain MC chromosome (NR_042460) was used as an outgroup (McKee et al., 2021). *Bartonella tribocorum* (KT32703, DQ480758, MH748138) was used as an outgroup for the housekeeping genes gltA, groEL, and rpoB (Nasereddin et al., 2014).

3.7 Fishers Test

To determine if *Bartonella* positive bugs are correlated with the area sampled, fishers test was performed (https://www.socscistatistics.com/tests/fisher/default2.aspx). For this approach, only samples that had high quality sequences for both, the 16S amplicon sequencing and the specific MLST, were used.

Therefore, an arbitrary rule was set, were all samples which retrieved at least one high quality sequence for the analysed markers were considered *Bartonella* positive.

For the test, the positive and negative samples of two different locations were compared, Las Cienegas National Conservation Area (LC) and University of Arizona Desert Station (TU), which were sampled in 2019.

4. Results

4.1 Evaluation of gel electrophoresis

Amplification of 16S rRNA gene produced visible bands for 78 (50.65%) samples, supposedly indicating presence of a *Bartonella* species. Visible products for gltA amplification were retrieved from 37 (24.03%) samples, rpoB amplification yielded 92 (59.74%) positive samples and groEL amplification provided an evidence of 47 (30.52%) positive samples. In *Figures 2-5* a single gel photo example for each of the housekeeping gene is shown.

All PCR products showing visible bands on gel were sequenced.

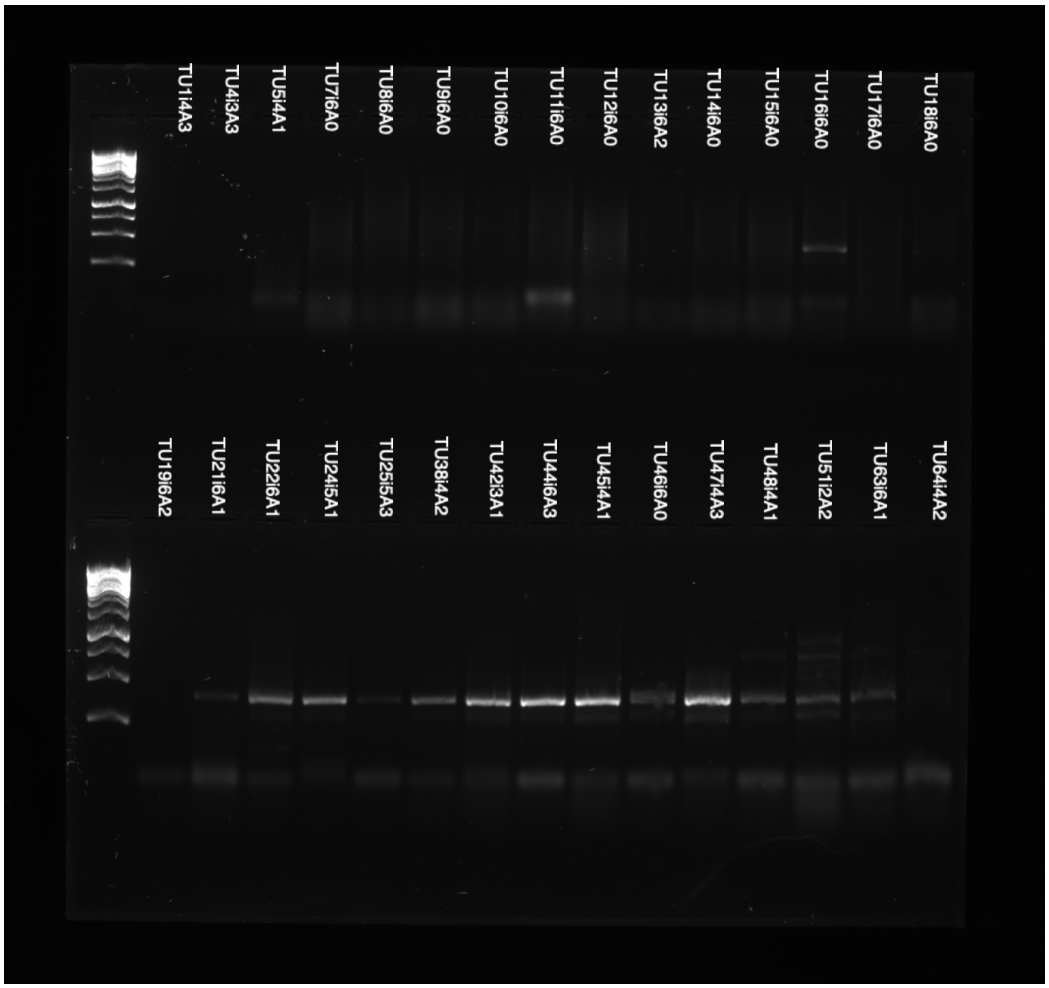

Figure 2: Visualization of 16S rRNA PCR products of 30 *T. rubida* samples, which were collected at the University of Arizona Desert Station in 2019

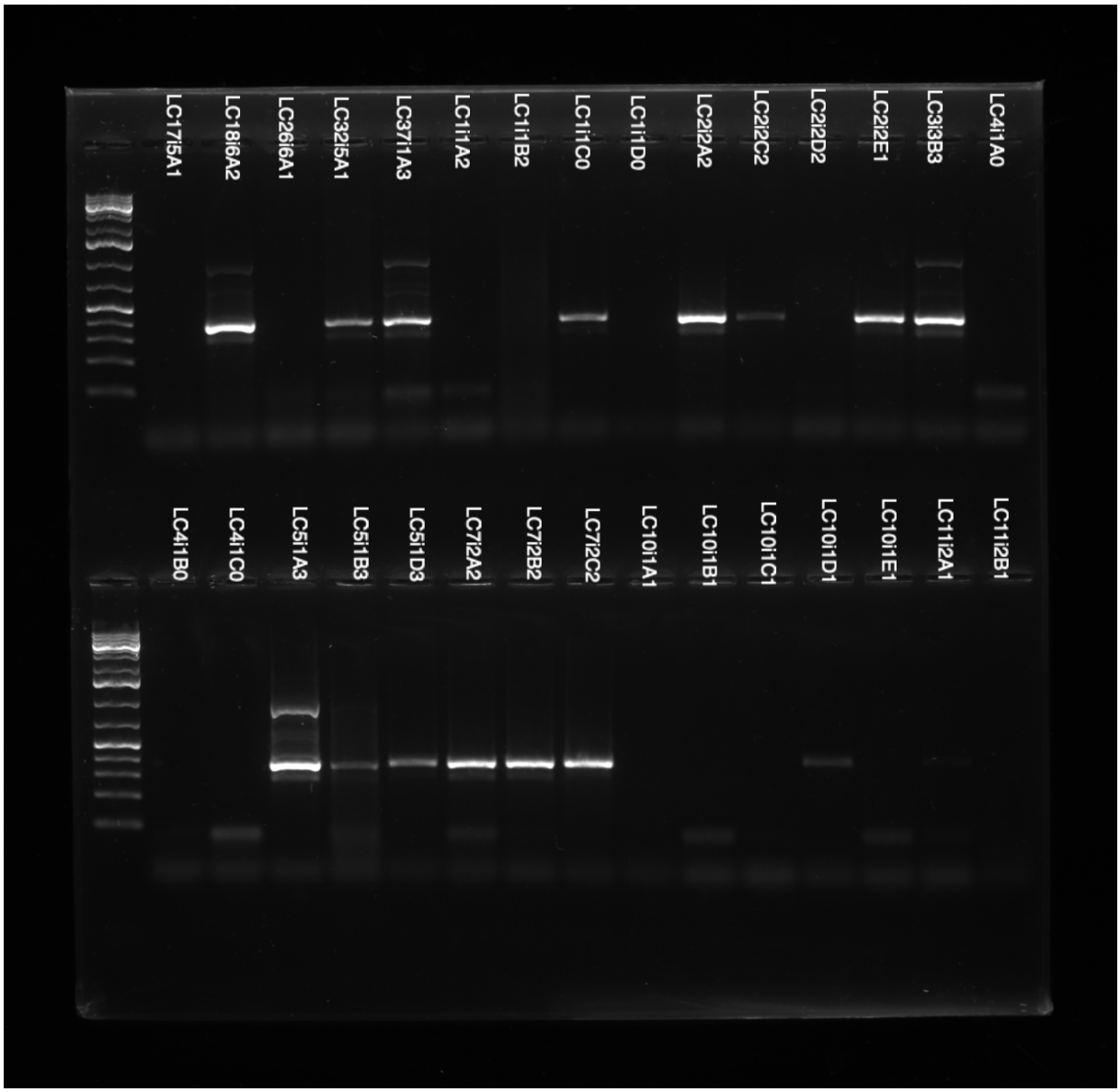

Figure 3: Visualization of gltA PCR products of 30 *T. rubida* samples that were collected in Las Cienegas Conservation Area in 2019

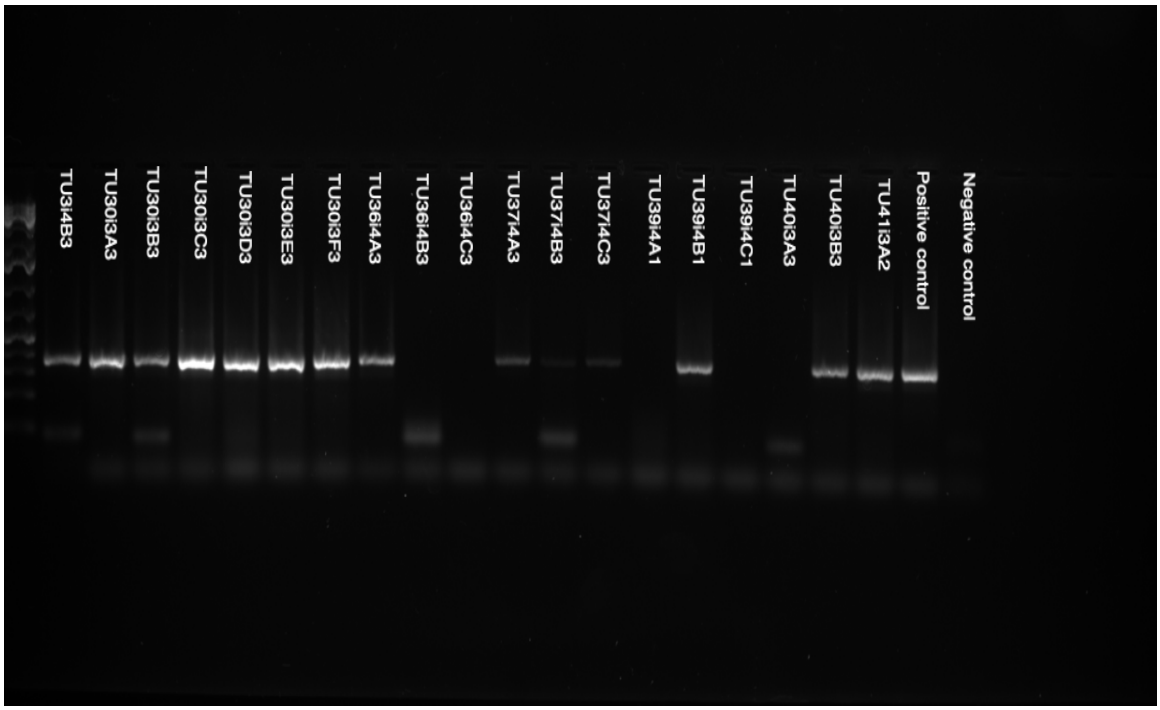

Figure 4: Visualization of rpoB PCR products of 19 *T. rubida* samples, which were collected at the University of Arizona Desert Station in 2019

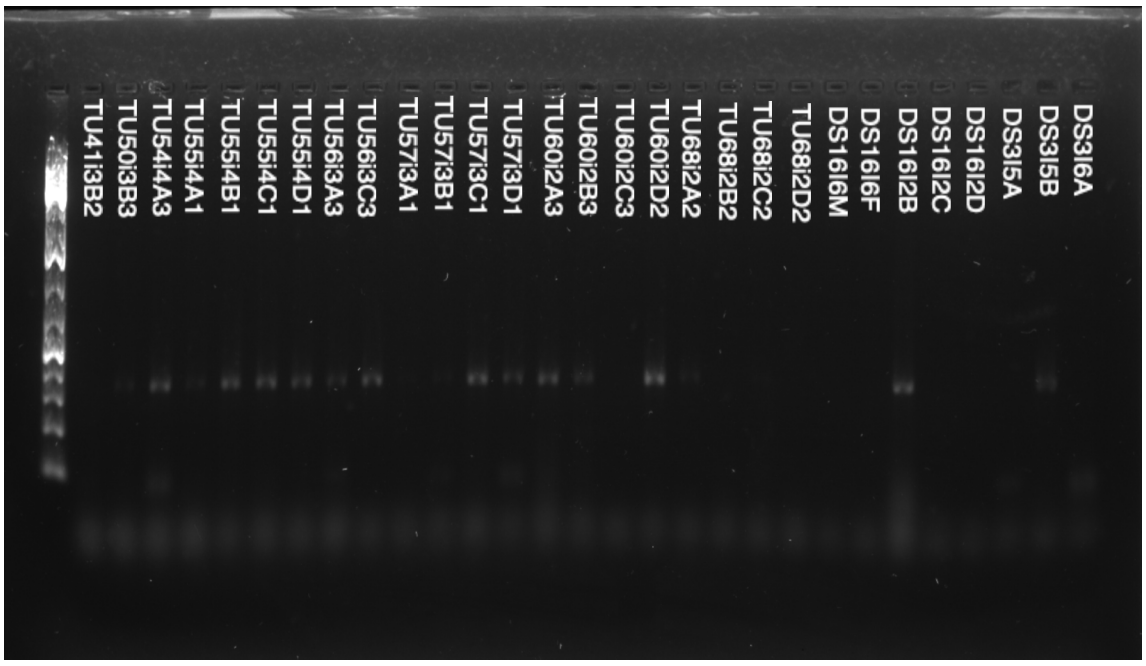

Figure 5: Visualization of groEL PCR products for 29 *T. rubida* samples, which were collected at the University of Arizona Desert Station in 2018 (8 samples) and 2019 (21 samples)

4.2 Molecular data evaluation

4.2.1 Comparison of the housekeeping genes

Only a fraction of sequenced PCR products yielded high quality sequences that could be used for further phylogenetic analyses (Figure 6). Majority of the sequences produced with the primers designed for a specific amplification of 16S rRNA gene of *Bartonellae* showed mixed signals in the chromatogram readings that hampered any further interpretation. Only 8.88% of the LC samples, 7.69% of the TU ones and 3,23% of the DS samples produced sequences with the first BLAST hit to the genus *Bartonella,* representing the worst result of the four genes tested.

Compared to the 16S rRNA primers, the rest of the primer pairs showed a reasonable specificity for the genus *Bartonella*. For the housekeeping gene gltA, the occurrence of *Bartonella* (based on the first BLAST hit) was 42.22% for LC, 6.41% for TU and 9.68% for DS. The third housekeeping gene rpoB, indicated 33.33% *Bartonella* positives among LC samples, 26.92% among TU samples and 35.48% among DS samples, which represents the best result of the genes tested. Finally, groEL showed *Bartonella* incidence in 37.78% of LC samples, 8.97% of TU samples and 19.35% of DS samples.

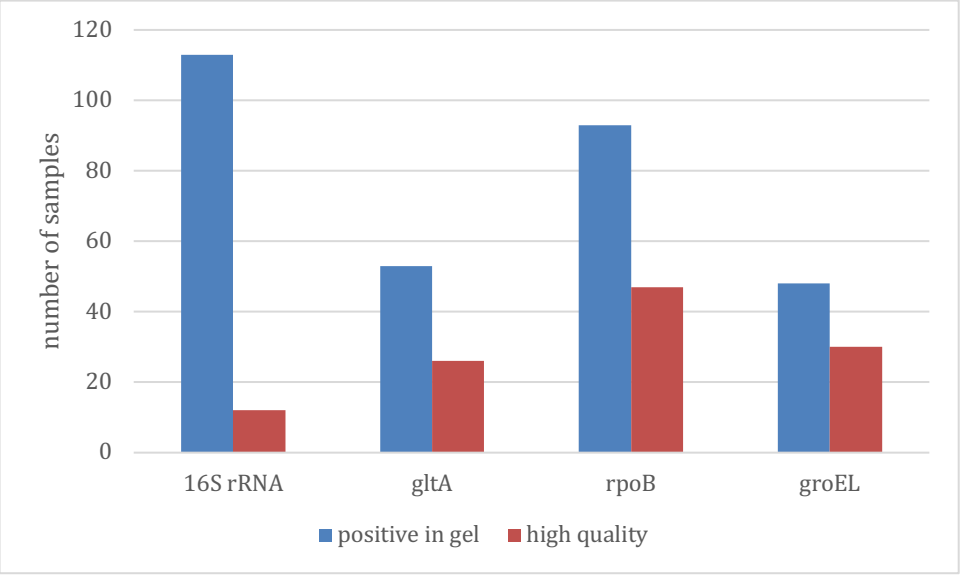

Figure 6: Number of visible bands vs. number of high quality sequences across all housekeeping genes.

As expected, the samples do differ in the year of sampling, which is observable in *Figure 7*. It is visible, for example, at the results of groEL, as there is a noticeable difference in the samples of TU and DS, which were sampled in the same location.

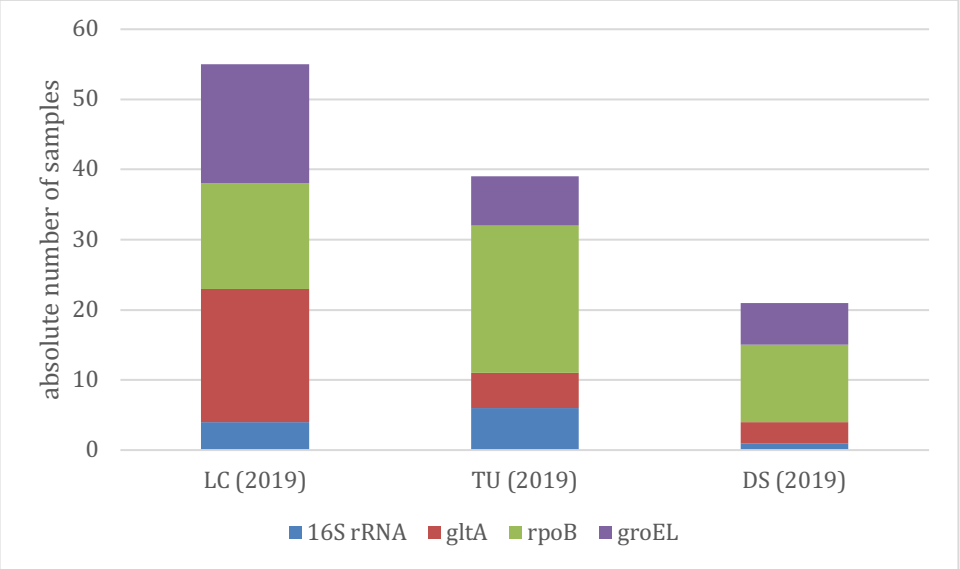

Figure 7: Absolute number of *Bartonella* positive samples across all housekeeping genes for each location and year of sampling. Thereby, LC indicates Las Cienegas National Conservation Area samples collected in 2019, TU and DS are indicating University of Arizona Desert Station samples collected in 2019 and 2018.

From the positive samples with high quality sequences, one can also assert that there is a difference for the larval stages of *Triatoma rubida* within the locations and years, which is illustrated in *Figure 8-10*. The second larval stages (L2) from Las Cienegas National Conservation Area show the highest *Bartonella* incidence. For the samples collected at the University of Arizona Desert Station in 2019, the highest *Bartonella* incidence was found among the third and fourth instars. From the same location but one year earlier collected samples, no significant statement can be provided. Ahead of every figure illustrating the larval stages, a table of the exact number of samples at a certain larval stage is given (Table 2-4).

Overall, the best indication of *Bartonella* species and subspecies within *T. rubida* is visible in rpoB for all larval stages collected at the University of Arizona Desert Station, and in the gltA gene for Las Cienegas National Conversation Area.

Table 2: Number of PCR products with high quality, collected from Las Cienegas National Conservation Area in 2019 at a certain larval stage. Thereby, L1 indicates the first larval instar increasing to L6 which is the adult form of *T. rubida*.

	16S rRNA	gltA	rpoB	groEL
L1	1	0	4	5
L2	2	11	5	8
L3	1	3	3	3
L4	0	1	1	1
L5	0	3	1	0
L6	0	0	1	0

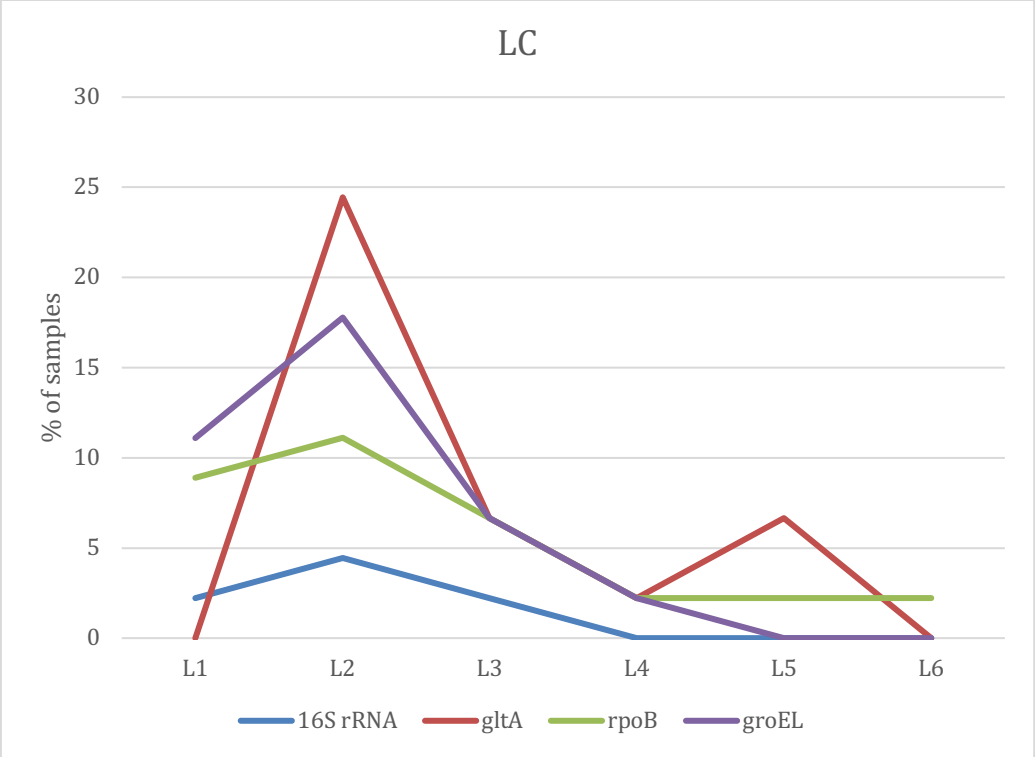

Figure 8: Percentage of *Bartonella* positive individuals in different ontogenetic stages collected from Las Cienegas National Conversation Area in 2019.

Table 3: Number of PCR products with high quality, collected from the University of Arizona Desert Station in 2019 at a certain larval stage. Thereby, L1 indicates the first larval instar increasing to L6 which is the adult form of *T. rubida*.

	16S rRNA	gltA	rpoB	groEL
L1	0	0	0	0
L2	0	0	0	0
L3	1	3	8	3
L4	4	0	11	4
L5	2	0	0	0
L6	0	2	2	0

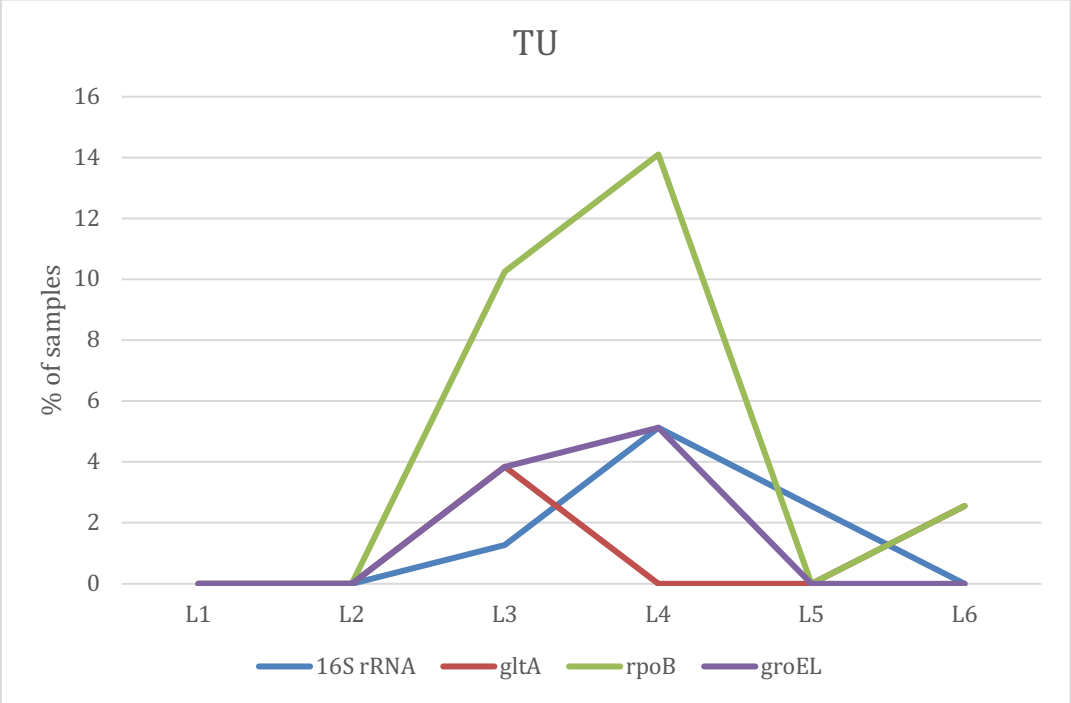

Figure 9: Percentage of Bartonella positive individuals in different ontogenetic stages collected from the University of Arizona Desert Station in 2019.

Table 4: Number of PCR products with high quality, collected from the University of Arizona Desert Station in 2018 at a certain larval stage. Thereby, L1 indicates the first larval instar increasing to L6 which is the adult form of *T. rubida*.

	16S rRNA	gltA	rpoB	groEL
L1	0	1	0	3
L2	0	0	1	2
L3	0	0	2	0
L4	0	0	0	0
L5	0	1	3	0
L6	1	1	5	1

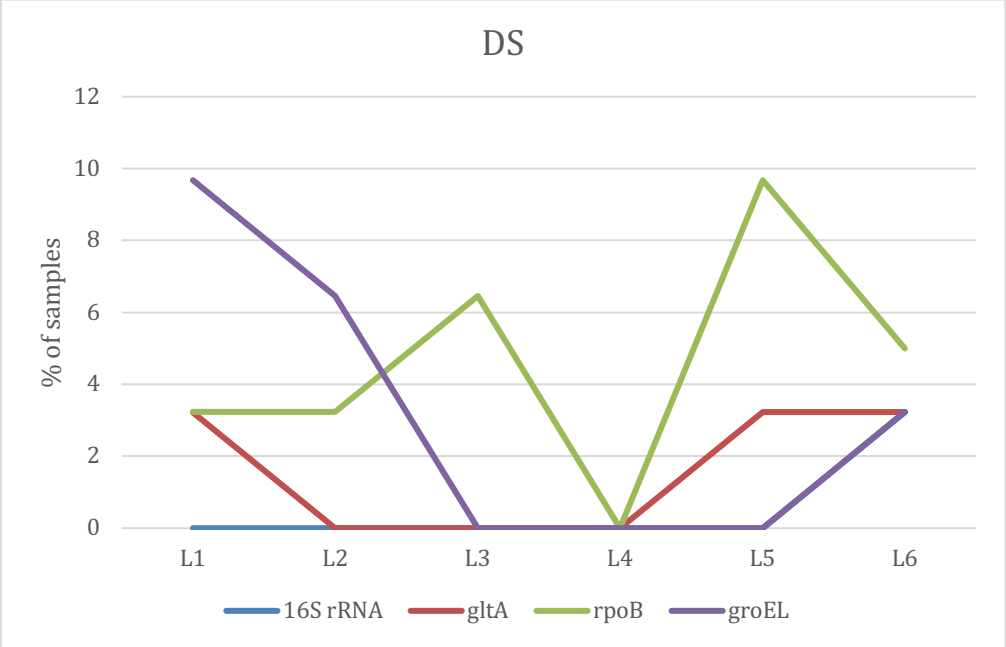

Figure 10: Percentage of *Bartonella* positive individuals in different ontogenetic stages collected from the University of Arizona Desert Station in 2018.

By taking a look at all samples with high quality of the four housekeeping genes, only 16 samples out of 154 were *Bartonella* positive. This happens due to the fact that the markers do not produce consistent results. By using the arbitrary rule, which is stated in the methodology, 84 out of 154 samples are considered *Bartonella* positive.

Considering both approaches, *Bartonella* specific MLST and nonspecific 16S rRNA gene amplification, 12 out of 123 samples are positive for all four housekeeping genes. Furthermore, 13 are positive for three housekeeping genes and 11 for two of them. In addition, also 11 samples are positive for 1 housekeeping gene.

Anyway, there are still 6 samples, which had a good result for the nonspecific 16S rRNA gene amplification but no result for the *Bartonella* specific MLST. All these results are summarized below (Table 5).

Table 5: Results of sequencing of LC and TU samples for both, nonspecific 16S rRNA high throughput amplicon sequencing and *Bartonella* specific MLST using four housekeeping genes. Results written in red are indicating high quality sequencing for both approaches. Sample name colours describe for how many housekeeping gene a result could be determined: blue = 4 housekeeping genes, yellow = 3 housekeeping genes, purple = 2 housekeeping genes, salmon pink= 1 housekeeping gene. Green indicates samples that were *Bartonella* positive for the nonspecific approach but negative for the specific MLST. LC designates samples collected from Las Cienegas National Conservation Area and TU indicates samples from the University of Arizona Desert Station.

	16S rRNA	gltA	rpoB	groEL
LC1i1A2	N.A.			
LC1i1B2	N.A.			
LC1i1C0	Bartonella vinsonii	Bartonella sp. na19103nm	Bartonella durdenii strain culsq-dd	Bartonella sp. SV06uk
LC1i1D0	Bartonella vinsonii		Bartonella durdenii strain culsq-dd	Bartonella sp. SV06uk
LC2i2A2	Bartonella vinsonii	Bartonella sp. na19103nm	Bartonella durdenii strain culsq-dd	Bartonella sp. SV06uk
LC2i2C2	Bartonella vinsonii	Bartonella sp. na19103nm	Bartonella durdenii strain culsq-dd	Bartonella sp. SV06uk
LC2i2D2	N.A.			
LC2i2E1	Bartonella sp. (Z69039)	Bartonella sp. na19103nm	Bartonella durdenii strain culsq-dd	Bartonella sp. SV06uk
LC3i3B2	Bartonella vinsonii subsp. berkhoffii	Bartonella sp. na19103nm	Bartonella durdenii strain culsq-dd	Bartonella sp. SV06uk
LC4i1A0	N.A.			
LC4i1B0	N.A.			
LC4i1C0	N.A.			
LC5i1A3	Bartonella vinsonii	N.A.	Bartonella durdenii strain culsq-dd	Bartonella sp. SV06uk
LC5i1B3	N.A.	Bartonella sp. na19233nm	Bartonella durdenii strain culsq-dd	Bartonella vinsonii
LC5i1D3	Bartonella vinsonii	Bartonella sp. na18990nm	Bartonella durdenii strain culsq-dd	Bartonella sp. SV06uk
LC7i2A2	Bartonella vinsonii subsp. berkhoffii	Bartonella sp. na19103nm	Bartonella durdenii strain culsq-dd	Bartonella sp. SV06uk
LC7i2B2	N.A.	Bartonella sp. na19103nm		Bartonella sp. SV06uk
LC7i2C2	Bartonella vinsonii subsp. berkhoffii	Bartonella sp. na19103nm		Bartonella sp. SV06uk
LC10i1A1				
LC10i1B1				
LC10i1C1				
LC10i1D1		N.A.		
LC10i1E1			Bartonella durdenii strain culsq-dd	
LC11i2A1	Bartonella vinsonii subsp. berkhoffii			
LC11i2B1				
LC11i2C1		Bartonella sp. na18990nm	Bartonella durdenii strain culsq-dd	

LC11i2D1		Bartonella sp. na19103nm	Bartonella vinsonii subsp. vinsonii	Bartonella vinsonii
LC13i3A3	Bartonella vinsonii subsp. berkhoffii	Bartonella sp. na18990nm	Bartonella durdenii strain culsq-dd	Bartonella sp. SV06uk
LC13i3B3	Bartonella vinsonii subsp. berkhoffii	Bartonella sp. na18990nm	Bartonella durdenii strain culsq-dd	Bartonella sp. SV06uk
LC14i4A2	Bartonella vinsonii subsp. berkhoffii	Bartonella sp. na18990nm	Bartonella durdenii strain culsq-dd	Bartonella sp. SV06uk
LC14i4B1	Uncultured Bartonella sp. clone DMS130418-RN4	Bartonella sp. na19103nm		
LC28i2A1	Bartonella vinsonii subsp. berkhoffii	Bartonella sp. na19103nm	Bartonella durdenii strain culsq-dd	
LC28i2B2	Bartonella sp. strain B32273	Bartonella sp. na19103nm	Bartonella durdenii strain culsq-dd	Bartonella sp. SV06uk
LC28i2C2	Bartonella vinsonii	Bartonella sp. na19103nm	Bartonella durdenii strain culsq-dd	Bartonella sp. SV06uk
LC33i2A3	N.A.	Bartonella sp. na19103nm		
LC33i2B3	N.A.			
LC33i2C3	N.A.			
TU2i4A3	BarG48:Q134tonella vinsonii		Bartonella durdenii strain culsq-dd	
TU2i4B3	Bartonella vinsonii		Bartonella durdenii strain culsq-dd	
TU3i4A3	Bartonella vinsonii		Bartonella durdenii strain culsq-dd	
TU3i4B3	Bartonella vinsonii		Bartonella durdenii strain culsq-dd	
TU30i3A3		Bartonella sp. Na97ro	Bartonella durdenii strain culsq-dd	
TU30i3B3		N.A.	Bartonella durdenii strain culsq-dd	
TU30i3C3			Uncultured Bartonella sp. clone Ben59	
TU30i3D3			Bartonella durdenii strain culsq-dd	
TU30i3E3		Bartonella sp. Na97ro	Bartonella durdenii strain culsq-dd	
TU30i3F3			Bartonella durdenii strain culsq-dd	
TU36i4A3			Candidatus Bartonella rudakovii isolate St490	
TU36i4B3				
TU36i4C3				
TU37i4A3	N.A.		Bartonella sp. strain 2015-247	
TU37i4B3	N.A.		Bartonella sp. strain 2015-247	
TU37i4C3	N.A.		Bartonella durdenii strain culsq-dd	
TU39i4A1	N.A.			
TU39i4B1	N.A.		Uncultured Bartonella sp. clone NB-1.1	
TU39i4C1	N.A.			
TU40i3A3	N.A.			
TU40i3B3	N.A.		Bartonella durdenii strain culsq-dd	
TU41i3A2	N.A.		Bartonella durdenii strain culsq-dd	
TU41i3B2	N.A.		Bartonella durdenii strain culsq-dd	
TU50i3B3	N.A.	N.A.	Candidatus Bartonella rudakovii isolate St490	Bartonella vinsonii
TU54i4A3	Bartonella sp. (Z69039)		Bartonella sp. M21D3	Bartonella vinsonii subsp. berkhoffii
TU54i4B2	Candidatus Bartonella rudakovii isolate St490	N.A.	Bartonella sp. AR15-3	Bartonella vinsonii subsp. berkhoffii
TU55i4A1	Candidatus Bartonella rudakovii isolate St490	Bartonella sp. ED377	Bartonella sp. M21D3	Bartonella vinsonii
TU55i4B1	Bartonella sp. (Z69039)	N.A.	Candidatus Bartonella rudakovii isolate St490	Bartonella vinsonii
TU55i4C1	Bartonella sp. (Z69039)		N.A.	Bartonella sp. B44
TU55i4D1	Bartonella sp. (Z69039)		Candidatus Bartonella rudakovii isolate St490	Bartonella vinsonii subsp. berkhoffii
TU56i3A3	Bartonella sp. (Z69039)	N.A.	Candidatus Bartonella rudakovii isolate St490	Bartonella vinsonii
TU56i3C3	Bartonella ancashensis strain 20.00		Candidatus Bartonella rudakovii isolate St490	
TU57i3A1			Bartonella sp. strain 2015-247	Bartonella sp. A202
TU57i3B1	Uncultured Bartonella sp. (AF467895)	N.A.	Candidatus Bartonella rudakovii isolate St490	Bartonella vinsonii subsp. berkhoffii
TU57i3C1	N.A.	N.A.	Candidatus Bartonella rudakovii isolate St490	Bartonella vinsonii subsp. berkhoffii
TU57i3D1	Bartonella sp. (Z69039)		Candidatus Bartonella rudakovii isolate St490	Bartonella vinsonii subsp. berkhoffii
TU60i2A3	Bartonella ancashensis strain 20.00	N.A.	Candidatus Bartonella rudakovii isolate St490	Bartonella vinsonii
TU60i2B3	Candidatus Bartonella rudakovii isolate St490	N.A.	Uncultured Bartonella sp. (KU175895)	
TU60i2C3	Bartonella bacilliformis	N.A.	Uncultured Bartonella sp. clone RR17	Bartonella vinsonii
TU60i2D2	Uncultured Bartonella sp. clone DMS130502-RN32		Candidatus Bartonella rudakovii isolate St490	Bartonella vinsonii
TU68i2A2				
TU68i2B2		N.A.	Uncultured Bartonella sp. clone NB-1.1	
TU68i2C2				
TU68i2D2	N.A.			
TU1i4A3		Bartonella sp. nm15586co		
TU4i3A3			Bartonella durdenii strain culsq-dd	
TU5i4A1				
TU7i6A0				
TU8i6A0			Bartonella vinsonii subsp. berkhoffii	
TU9i6A0				
TU10i6A0				
TU11i6A0				
TU12i6A0				
TU13i6A2				

TU14i6A0				
TU15i6A0			Bartonella durdenii strain culsq-dd	
TU16i6A0	N.A.			
TU17i6A0				
TU18i6A0				Bartonella vinsonii subsp. berkhoffii
TU19i6A2				
TU21i6A1	N.A.			
TU22i6A1	Bartonella sp. (Z69039)			
TU24i5A1	Bartonella sp. (Z69039)			
TU25i5A3	Bartonella sp. strain E1 B23987			
TU38i4A2	N.A.			
TU42i3A1	N.A.		Bartonella durdenii strain culsq-dd	
TU44i6A3	Bartonella sp. strain B40899	Bartonella sp. Na97ro	Bartonella durdenii strain culsq-dd	
TU45i4A1	Bartonella sp. strain C1phy		Bartonella durdenii strain culsq-dd	Bartonella vinsonii subsp. berkhoffii
TU46i6A0	Bartonella sp. (Z69039)	Bartonella sp. Na97ro	Uncultured Bartonella sp. clone RR17	
TU47i4A3	N.A.			
TU48i4A1	N.A.			
TU51i2A2	N.A.			
TU63i6A1				
TU64i4A2	N.A.			
TU65i3A2				
TU67i3A2				
TU73i3A0	N.A.	Bartonella sp. ED377	Bartonella sp. M21D3	
TU74i4A1	Bartonella sp. strain C1phy			
LC12i2A2	Bartonella vinsonii subsp. berkhoffii	Bartonella sp. na18990nm		
LC15i5A3	Bartonella sp. (Z69039)	Bartonella sp. na19103nm		
LC16i5A1	Bartonella sp. strain T-837 B42973	Bartonella sp. na19103nm		
LC17i6A1	N.A.			
LC18i6A2	N.A.	Bartonella sp. na19103nm	Bartonella durdenii strain culsq-dd	
LC26i6A1	N.A.			
LC32i5A1	N.A.	Bartonella sp. na19103nm	Bartonella durdenii strain culsq-dd	
LC37i1A3	Bartonella vinsonii subsp. berkhoffii		Bartonella durdenii strain culsq-dd	Bartonella sp. SV06uk

For the completeness another table was made to visualize high quality sequences of DS samples. The results can be observed in *Table 6*.

Table 6: Results of sequencing of DS samples for *Bartonella* specific MLST. Results written in red are indicating high quality sequencing for both approaches. Sample name colours describe for how many housekeeping gene a result could be determined: blue = 4 housekeeping genes, yellow = 3 housekeeping genes, purple = 2 housekeeping genes, salmon pink= 1 housekeeping gene.

DS16I6M	Bartonella vinsonii subsp. berkhoffii		Bartonella sp. M21D3	
DS16I6F	Uncultured Bartonella sp. clone MU6/KCF21		Candidatus Bartonella rudakovii isolate St490	Bartonella vinsonii subsp. berkhoffii
DS3I3A	Bartonella vinsonii	N.A.	Bartonella sp. M21D3	
DS3I3B	Bartonella vinsonii	N.A.	Bartonella sp. strain 2015-247	
DS3I3C	Bartonella vinsonii	N.A.	Candidatus Bartonella rudakovii isolate St490	
DS16I2A	Bartonella vinsonii		Bartonella durdenii strain culsq-dd	Bartonella vinsonii
DS16I2B	Bartonella vinsonii subsp. arupensis		Bartonella durdenii strain culsq-dd	
DS16I2C	Bartonella vinsonii		Bartonella durdenii strain culsq-dd	Bartonella vinsonii subsp. berkhoffii
DS16I2D	Bartonella vinsonii		Bartonella durdenii strain culsq-dd	Bartonella vinsonii subsp. berkhoffii
DS3I5A	Candidatus Bartonella rudakovii isolate St490	Bartonella sp. ED377	Bartonella sp. M21D3	
DS3I5B			Bartonella sp. strain 2015-247	
DS3I6A	Bartonella vinsonii subsp. berkhoffii	N.A.	Bartonella sp. M21D3	
DS3I6B	Bartonella sp. (Z69039)	Bartonella sp. ED377	Bartonella sp. strain 2015-247	
DS16I1A	Bartonella vinsonii		Bartonella durdenii strain culsq-dd	Bartonella vinsonii subsp. arupensis
DS16I1B	Bartonella vinsonii		Bartonella durdenii strain culsq-dd	
DS16I1D	Bartonella vinsonii			
DS16I1E	Bartonella vinsonii		Bartonella durdenii strain culsq-dd	Bartonella vinsonii
DS16I1F	Bartonella vinsonii	Bartonella sp. nm15586co	Bartonella durdenii strain culsq-dd	Bartonella vinsonii subsp. berkhoffii
DS16I5A	Bartonella vinsonii	Bartonella sp. nm15586co	Bartonella durdenii strain culsq-dd	Bartonella vinsonii subsp. berkhoffii
DS3I5	Candidatus Bartonella krasnovii strain OE 1-1		Bartonella sp. M21D3	
DS3I6	Bartonella vinsonii subsp. berkhoffii	Bartonella sp. ED377	Bartonella sp. M21D3	
DS13I6	Bartonella vinsonii			
DS5I6A	Bartonella vinsonii		Bartonella durdenii strain culsq-dd	Bartonella vinsonii
DS5I6B	Bartonella vinsonii			
DS12I6M	Bartonella sp. strain C5rat			
DS18I6	Bartonella vinsonii		Bartonella sp. strain 2015-247	
DS12I6F	Bartonella vinsonii		Candidatus Bartonella rudakovii isolate St490	Bartonella vinsonii subsp. berkhoffii
DS15I6	Bartonella vinsonii subsp. berkhoffii		Bartonella durdenii strain culsq-dd	Bartonella vinsonii subsp. berkhoffii
DS6I6	Bartonella sp. (Z69039)		Bartonella sp. strain 2015-247	
DS5I6	Uncultured Bartonella sp. clone MU6/KCF21		Candidatus Bartonella rudakovii isolate St490	
DS3M-A	Bartonella vinsonii		Bartonella sp. M21D3	

4.2.2 Detection of *Bartonella* sp.: comparison of *Bartonella* specific MLST and nonspecific 16S rRNA gene amplification using Illumina sequencing

To compare targeted (*Bartonella* specific) and untargeted approaches, the results from the high throughput 16S rRNA amplicon sequencing, done by supervisor's laboratory in 2018, were used. Detailed information on the data set is provided, as already stated in 3.1, in the appendix in *Table 3*.
In total, the team collected 87 samples at the University of Arizona Desert Station (UADS) and 71 samples in the Las Cienegas National Conservation Area (LCNCA).

For the comparison, only samples with *Bartonella* OTU 42 comprising more than 10 reads, which are overlapping with the samples analysed with MLST were utilized.
Out of these, 30 samples were collected at the University of Arizona Desert Station and 23 samples were gathered in the Las Cienegas National Conservation Area. Therefore, 53 out of 158 samples were positive for *Bartonella*, indicating a better result compared to the samples analysed with MLST.

By comparing the localities, it is visible that the samples, which were analysed with the specific MLST gene amplification, had a higher *Bartonella* incidence for samples collected from LC. However, for samples collected from TU, the non-specific 16S rRNA gene amplification indicates a better result. *Table 7* shows the comparison of the two approaches in percentage.

	% of *Bartonella* positive samples	% of LC	% of TU
Specific MLST	24,68%	44,44%	23,08%
Non-specific 16S rRNA amplicon sequencing	33,54%	32,39%	34,48%

Table 7: Comparison of *Bartonella* positive samples for two sequencing methods in percentage.

In *Figure 11* the comparing of the larval stages of the *Bartonella* positive samples from different locations, is observable. It is noticeable that the samples collected in Las Cienegas National Conservation Area have a higher *Bartonella* incidence for the larval stage L2. For the samples gathered from the University of Arizona Desert Station, the highest incidence is found in larval stage L3. This is in agreement with the results that were obtained from the samples analysed with specific MLST.

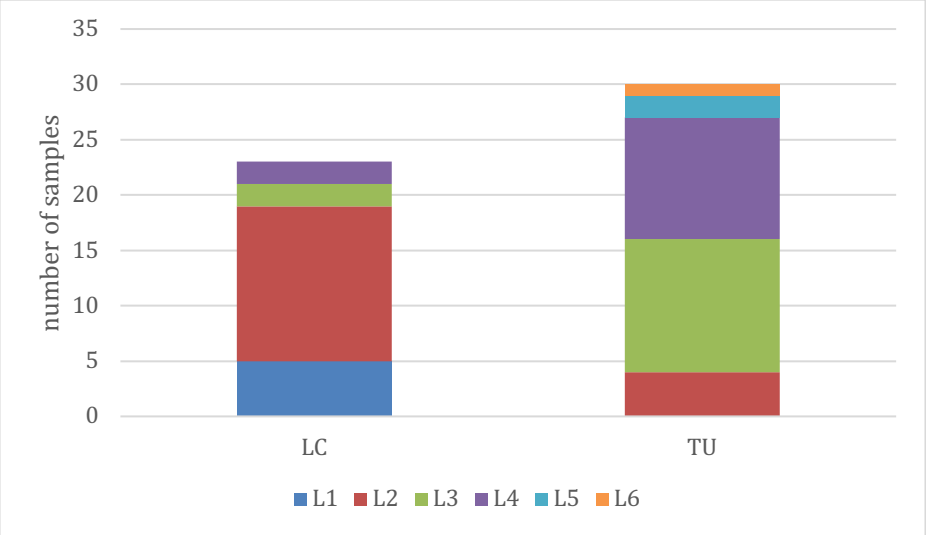

Figure 11: Comparison of larval stages for *Bartonella* positive samples analysed with non-specific 16S rRNA amplicon sequencing

4.3 Evaluation of Fishers exact test

For the Fishers exact test, positive and negative samples collected from LC and TU were used. The fishers exact test statistic value was found to be 0.0368, which indicates that the result is significant at the confidence interval of 95%. This shows that Bartonella infection is strongly associated with a sampling site. The complete results of the Fishers exact test are observable in *Table 9*.

Table 8: Results of Fishers exact test for LC and TU samples.

	positive	negative	Marginal Row Totals
LC	20	3	23
TU	18	12	30
Marginal Column Totals	38	15	53 (Grand Total)

4.4 BLAST based analyses

Based on the first BLAST hit against nr database, the majority of 16S rRNA sequences retrieved in this work were identified as *Bartonella vinsonii*. The majority of gltA and groEL sequences were identified into the genus level as *Bartonella sp. Na19103nm* and *Bartonella* sp. SV06uk, respectively. *Bartonella durdenii strain culsq-dd*, was the most prevalent first BLAST hit for the rpoB sequences. This is visualized in *Figure 12* below.

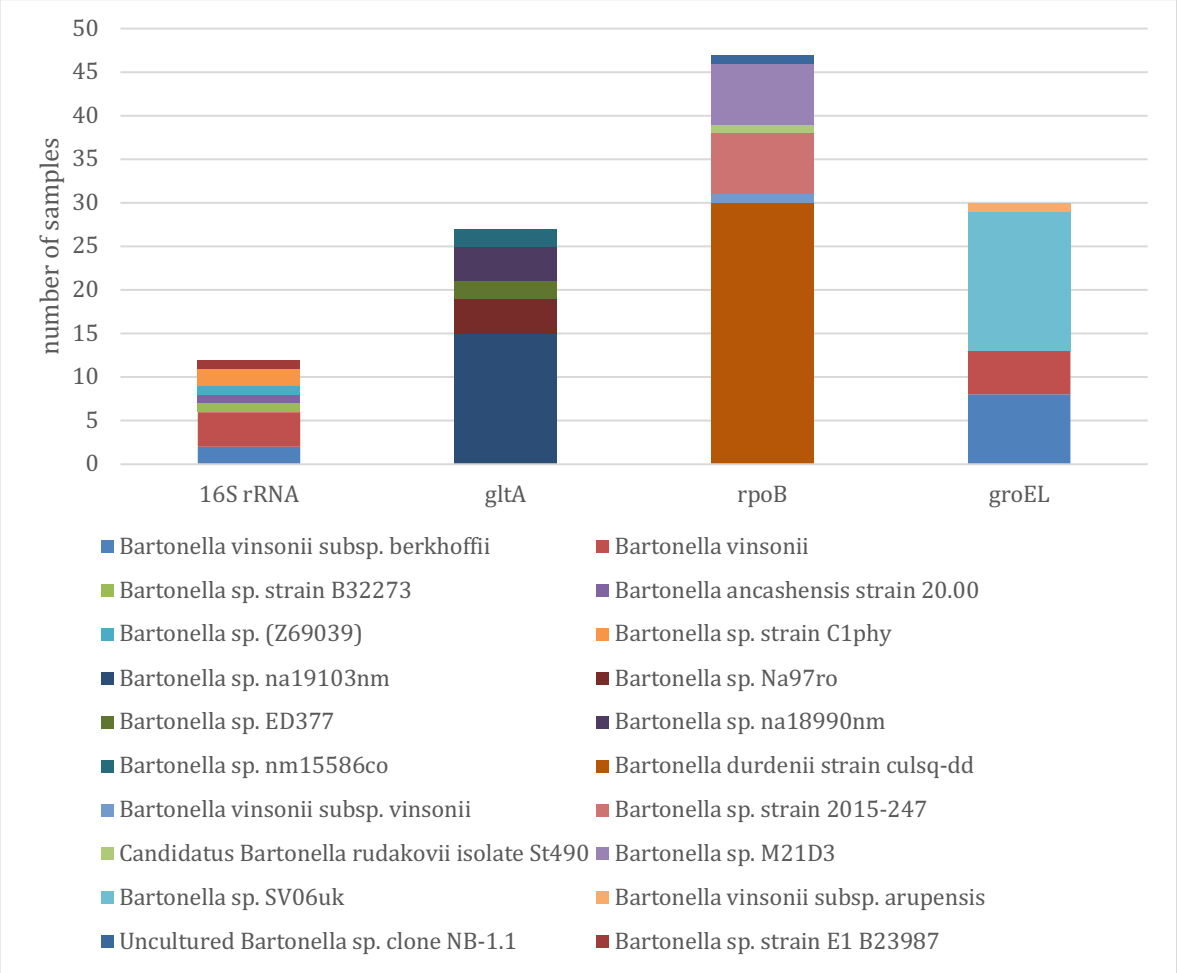

Figure 12: Sequencing results of high-quality sequences based on first BLAST hit, indicating which *Bartonella* species forms the majority for each housekeeping gene. The outcome of the sequencing shows that the highest quality of sequences can be found for rpoB, whereas the lowest is revealed for 16S rRNA.

4.5 Phylogenetic analyses

For the analyses of 16S rRNA gene matrix, 12 samples and 13 genera revealed multiple origins of *Bartonella* infection in the analyzed *T. rubida.* However, the tree does not show high bootstrap supports and contains unresolved relationships among several species such as *Bartonella grahamii, Bartonella washoenis, Uncultured Bartonella sp. Clone and Bartonella rattimassiliensis* (Figure 13). Analyses with other housekeeping genes produced more supported topologies.

Figure 13 illustrates the phylogenetic tree of the housekeeping gene 16S rRNA. It is observable that the majority of the LC samples are clustering with *Bartonella rattimassiliensis*, whereas the TU samples are clustering with *Bartonella vinsonii*, *Bartonella rochalimae* and *Bartonella clarridgeiae*. In addition, it can be recognized that only three samples from the Las Cienegas Conservation Area have a stronger support (<60%).

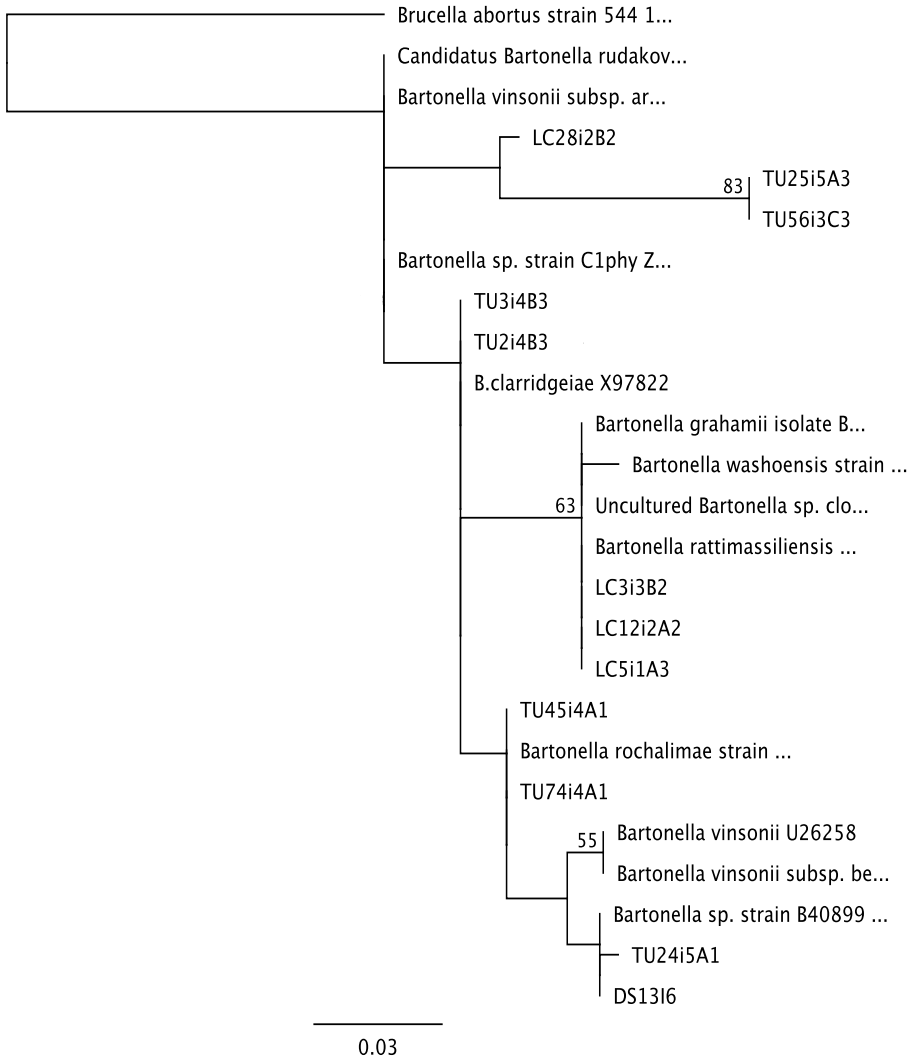

Figure 13: Phylogenetic analysis of 16S rRNA gene fragments retrieved from 12 *Triatoma rubida* individuals, showing multiple origins of *Bartonella* uptake. *Brucella abortus* was used as an outgroup. Bootstrap values above 50 are shown. In the graphic LC is indicating samples collected at Las Cienegas National Conservation Area in 2019. TU and DS are samples collected at the University of Arizona Desert Station in 2019 (TU) and 2018 (DS).

In the phylogenetic tree of the housekeeping gene gltA, which is shown in *Figure 14*, it is noticeable that the majority of the samples clustered into two different main clusters. For this analysis, 26 samples and 19 genera were used. By looking at some nodes no information about the evolution can be given anymore due to polytomous behaviour. By taking a look on the branch with 98 support, most are clustering with *Bartonella vinsonii*. It is also observable that the LC samples are creating a monophyletic cluster.

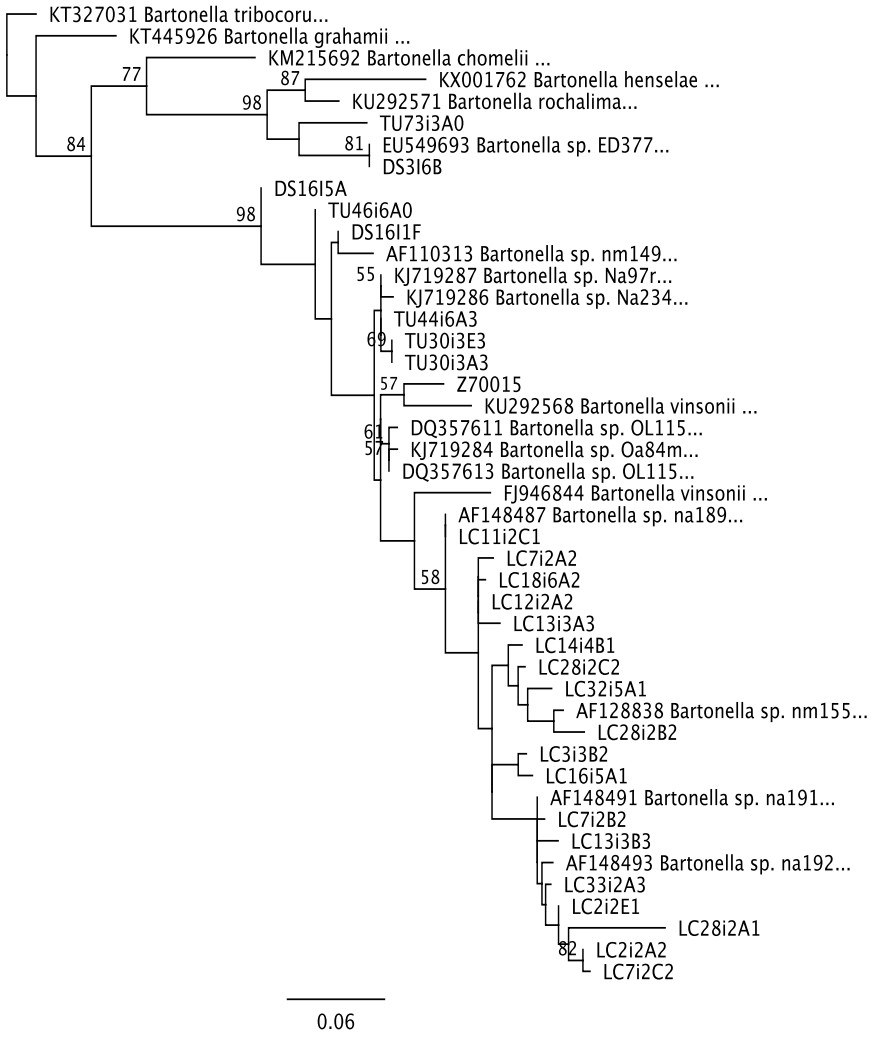

Figure 14: Phylogenetic analysis of gltA *Bartonella* sequences from 26 *Triatoma rubida* samples, showing that the phylogenetic origin of bacteria might be specific to the sites sampled in this study. *Bartonella tribocorum* was used as an outgroup. Bootstrap values above 50 are ahown. LC is indicating samples collected at Las Cienegas National Conservation Area in 2019. TU and DS are samples collected at the University of Arizona Desert Station in 2019 (TU) and 2018 (DS).

Analyses of rpoB gene matrix consisting of 47 samples and 12 genera are demonstrated in *Figure 15*. It is shown that there are two main branches, *Bartonella clarridgeiae* and *Bartonella vinsonii*. Furthermore, it can be detected that all samples from Tucson are clustering with *Bartonalla clarridgeiae* and *Bartonella vinsonii*, whereas LC samples only cluster with *B. vinsonii*. Only for closely related genera, both main clusters have a strong support over 90%. By taking a look at the nests, no specific pattern is observable

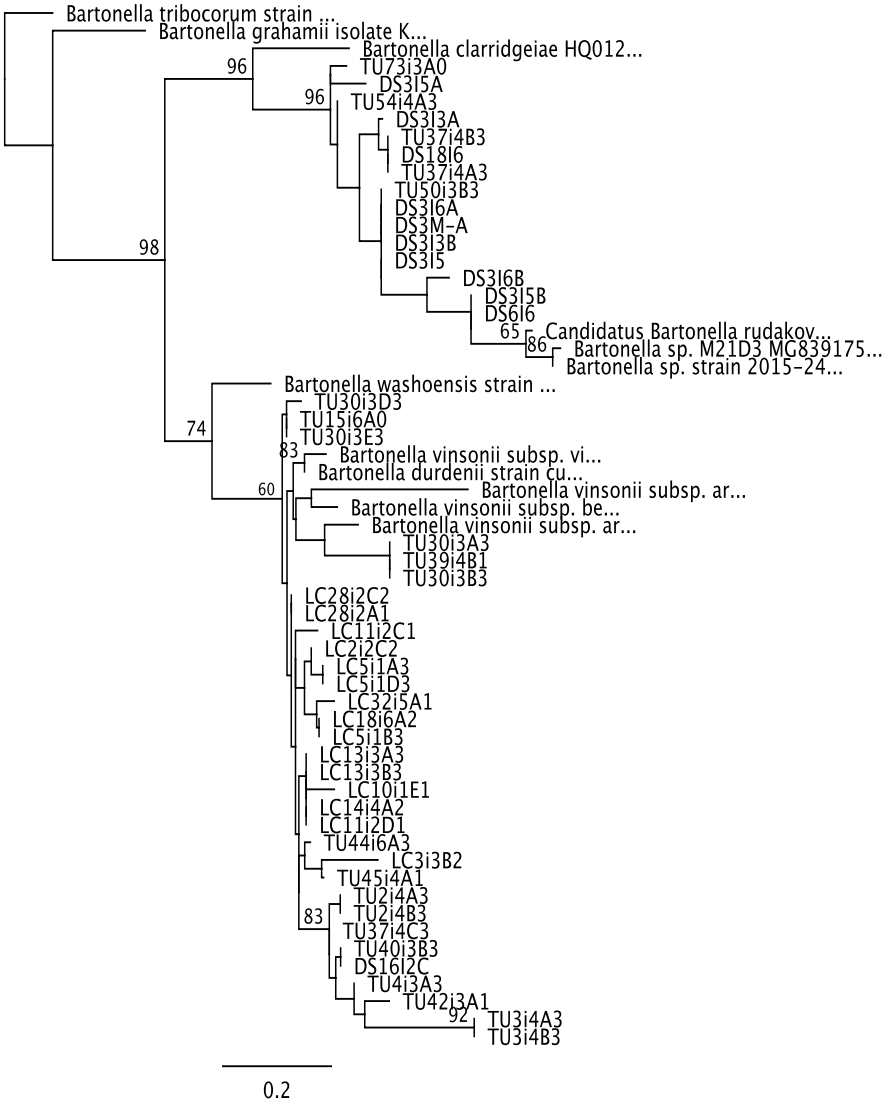

Figure 15: Phylogenetic analysis of rpoB for 47 *Triatoma rubida* samples, indicating multiple origins of *Bartonella* uptake. *Bartonella tribocorum* was used as an outgroup. Bootstrap values above 55 are shown. LC is indicating samples collected at Las Cienegas National Conservation Area in 2019. TU and DS are samples collected at the University of Arizona Desert Station in 2019 (TU) and 2018 (DS)

Figure 16 illustrates the phylogenetic tree for the housekeeping gene *groEL using 30 Triatoma rubida samples and 9 genera.* It is noticeable that there are two main branches, *Bartonella vinsonii* and *Bartonella vinsonii subsp. arupensis*. Besides that, it is shown that the DS and TU samples, which were collected from the same location, do all belong to *Bartonella vinsonii subsp. berkhoffi,* whereas the samples from Las Cienegas Conservation Area are closer related to *Bartonella grahamii*.

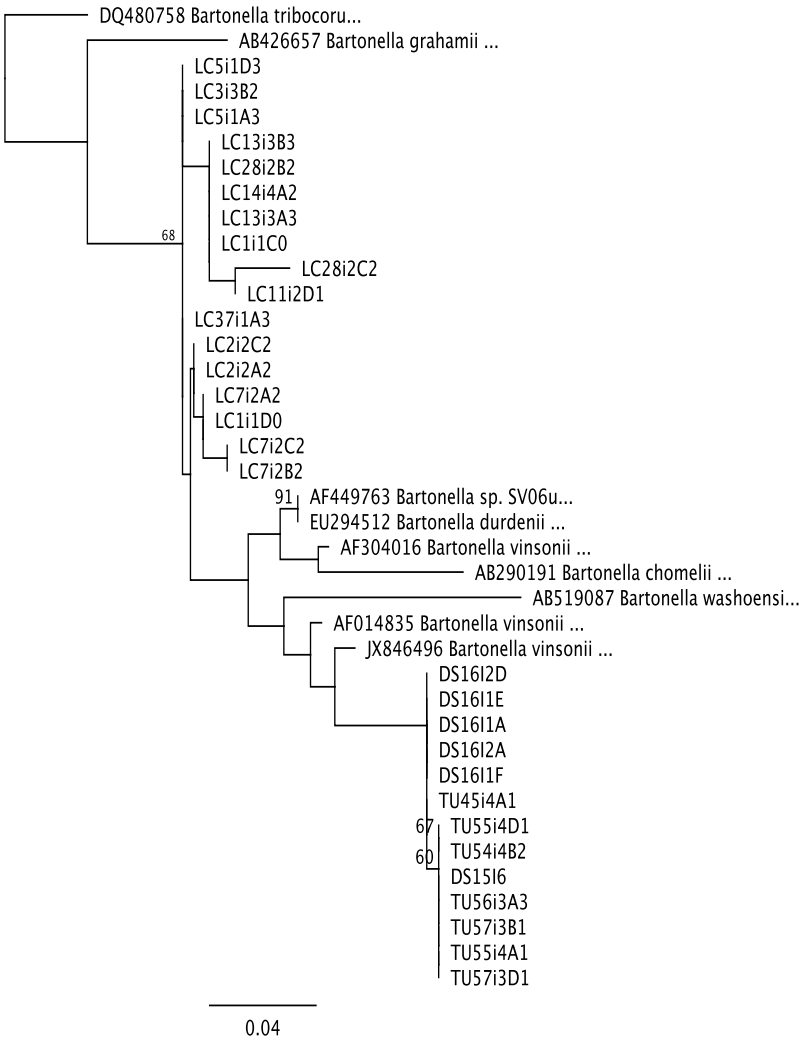

Figure 16: Phylogenetic analysis of groEL for 30 *Triatoma rubida* individuals, indicating that the phylogenetic origin might be specific to the sites samples in this study. *Bartonella tribocorum* was used as an outgroup. Bootstrap values above 55 are shown. LC is indicating samples collected at Las Cienegas National Conservation Area in 2019. TU and DS are samples collected at the University of Arizona Desert Station in 2019 (TU) and 2018 (DS).

5. Discussion

Triatominae are becoming a strong health concern in the United States, as they cause arduous allergic reactions due to their bites and are potential vectors for Chagas disease. Kissing bugs distribute in many areas of the southern United States, such as San Diego, Phoenix and Tucson (Klotz et al., 2014). Due to global warming, a further geographic distribution of kissing bug is very presumable, which is concerning as they are able to get in contact with other pathogens (Vieira et al., 2018). There are many different factors which may influence Triatomine vectors for transmitting different pathogens to human and pets.

The goal of this thesis was to evaluate the phylogenetic diversity of *Bartonella* associates in *T. rubida* samples originating from Arizona.

In this analysis, 16S rRNA did produce the most positive. Even though the primers should be specific to the genus, further sequencing revealed that most of the products were not recognized as *Bartonella*. For the quality of sequences, rpoB is suited best as molecular marker. The reason why for some markers lower number of sequences were retrieved might be that DNA abundance differs for the samples, if multiple species are present. Additionally, there could be an amplification bias towards some species due to their annealing affinity (Kosoy et al., 2018).
Two different methods were compared in this study, 16S rRNA amplicon sequencing and MLST. The 16S rRNA amplicon sequencing is used to detect an overall diversity, whereas MLST with specific primers is utilized to distinguish between related species (Galan et al., 2016). Therefore, MLST is the more sensitive choice. This explains why the percentage of *Bartonella* positive samples is slightly higher for samples using non-specific amplicon sequencing compared to the samples with specific MLST.

It has been previously shown that Triatomine bugs may acquire *Bartonella* from the packrat, *N. albigula*. Furthermore, it could be possible that *Bartonella* can not only be acquired from the bloodmeal of the packrat but also it can be transmitted from the Triatomines. In addition, *Bartonella* is an active part of *Triatoma* microbiomes, as some vertebrate pathogens in blood-sucking arthropods have evolved into symbionts.

Therefore, horizontal transmission might be a distinct mode of acquiring *Bartonella* symbionts (Brown et al., 2020).

Furthermore, the phylogenetic analysis indicated that there is a variety of different *Bartonella* species within the dataset. The data shows that ontogeny, geographic origin and different years of collection of *T. rubida* influences the *Bartonella* uptake from vertebrate hosts, which confirms previous studies' results (Brown et al., 2020). Low supports for presented topologies have been found as some sequences were too short. Another reason on why the trees show different *Bartonella* origins is that different genes retain different amount of information. Therefore, some are very conservative, and the stain could not be recognized, and some are less conservative. From this data, the best phylogenetic tree was obtained from the housekeeping gene *gltA*. Therefore, *gltA* is the best marker for very short sequences. One of the most frequent species found was *Bartonella vinsonii*, especially for samples collected in Tucson. This result can also be observed in Brown et al. (2020), where nearly all samples collected in Tucson had their origin in *Bartonella vinsonii*. Brown et al. (2020) was able to detect one species in *T. rubida,* whereas this study shows that there is a higher diversity of *Bartonella* species among this kissing bug species. In general, *Bartonella vinsonii* contains three major subspecies, *B. vinsonii subsp. arupensis, B. vinsonii subsp. vinsonii* and *B. vinsonii subsp. berkhoffii* (NCBI Taxonomy Browser). The second abundant species found in the dataset was *Bartonella clarridgeiae.* This species is known to be involved in the cat scratch disease (Logan et al., 2019).

This study shows that there is a broader diversity of species among *T. rubida* than currently known, at least regarding US species. To verify more conclusion on all Triatomine species, more studies would be needed. Nevertheless, *Bartonella* infections in kissing bugs should be taken as a serious health concern and more investigations should be performed.

6. Conclusion

Triatominae are the main vector transmitting *T. cruzi* causing Chargas disease in humans and canines. This study describes *Triatoma rubida* as a potential vector of bacterial pathogens from the genus *Bartonella* adding on great public concern about this vector. It is confirmed that locality, ontogeny, and the year of collection are the three main factors for *Bartonella* infections. This research shows that there are different *Bartonella* species found in the *T. rubida* samples, such as *Bartonella vinsonii* and *Bartonella clarridgeiae*. For the housekeeping gene gltA, the majority of all sequences yielded very high similarity with *Bartonella vinsonii*, with a prevalence of 92,31%. Considering rpoB, samples collected in Tucson clustered with *Bartonella vinsonii subsp berkhoffi,* whereas the samples from Las Cienegas Conservation Area were closer related to *Bartonella grahamii*.

Overall, this study shows that there is a broader diversity of *Bartonella* in *T. rubida* than shown previously. It is observable that there are at least two species of *Bartonella* in the presented dataset. Furthermore, it is demonstrated, that there is a high prevalence of *Bartonella* in the *T. rubida* populations in Arizona.
Future research might focus on finding *Bartonella* in vertebrates and specify the characteristics of *Bartonella* infections. At this point, the transmission remains questionable as there is no data on *Bartonella* in Triatominae salivary glands or faeces.

7. References

- Bayão T.S., Cupertino M.D.C., Mayers N.A.J., and Siqueira-Batista R. (2020). A systematic review of the diagnostic aspects and use of *Trypanosoma rangeli* as an immunogen for *Trypanosoma cruzi* infection. Rev Soc Bras Med Trop. 2020 Sep 11;53:e20190608. doi: 10.1590/0037-8682-0608-2019.
- Bern C., Kjos S., Yabsley M.J., and Montgomery S.P. (2011). *Trypanosoma cruzi* and Chagas' Disease in the United States. Clin Microbiol Rev. 2011 Oct;24(4):655-81. doi: 10.1128/CMR.00005-11.
- Bern, C., Messenger, L. A., Whitman, J. D., & Maguire, J. H. (2019). Chagas Disease in the United States: a Public Health Approach. *Clin Microbiol Rev*. 2019;33(1):e00023-19. doi:10.1128/CMR.00023-19
- Billeter, S.A., Levy, M.G., Chomel, B.B., and Breitschwerdt, E.B. (2008). Vector transmission of *Bartonella* species with emphasis on the potential for tick transmission. Med Vet Entomol. 2008 Mar;22(1):1-15. doi: 10.1111/j.1365-2915.2008.00713.x.
- Bonney, K.M. (2014). Chagas disease in the 21st century: a public health success or an emerging threat? Parasite. 2014;21:11. doi: 10.1051/parasite/2014012.
- Brook C.E., Dobson A.P., Osikowicz L.M., Ranaivoson H.C., Zhu Q., Kosoy M.Y., and Dittmar K. (2015). *Bartonella spp.* in fruit bats and blood-feeding Ectoparasites in Madagascar. PLoS Negl Trop Dis. 2015 Feb 23;9(2):e0003532. doi: 10.1371/journal.pntd.0003532.

- Brown, J.J., Rodríguez-Ruano, S.M., Poosakkannu, A., Batani, G., Schmidt, J.O., Roachell, W., Zima Jr, J., Hypša V., and Nováková, E. (2020). Ontogeny, species identity, and environment dominate microbiome dynamics in wild populations of kissing bugs (Triatominae). Microbiome. 2020 Oct 11;8(1):146. doi: 10.1186/s40168-020-00921-x.
- Buffet, J.P., Kosoy, M., and Vayssier-Taussat, M. (2013). Natural history of B*artonella*-infecting rodents in light of new knowledge on genomics, diversity and evolution. Future Microbiol. 2013 Sep;8(9):1117-28. doi: 10.2217/fmb.13.77.
- Chomel, B.B., and Kasten R.W. (2010). Bartonellosis, an increasingly recognized zoonosis. J Appl Microbiol. 2010 Sep;109(3):743-50. doi: 10.1111/j.1365-2672.2010.04679.x.
- Cohen J.E., and Gürtler R.E. (2001). Modeling Household Transmission of American Trypanosomiasis. Science 2001 Jul 27;293(5530):694-8. doi: 10.1126/science.1060638.
- Da Mota, F.F., Marinho, L.P., Moreira, C.J.D.C., Lima, M.M., Mello, C.B., Garcia, E.S., Carels, N., and Azambuja, P. (2012). Cultivation-independent methods reveal differences among bacterial gut microbiota in triatomine vectors of Chagas disease. PLoS Negl Trop Dis. 2012;6(5):e1631. doi: 10.1371/journal.pntd.0001631.
- Díaz S., Villavicencio B., Correia N., Costa J., and Haag K.L. (2016). Triatomine bugs, their microbiota and *Trypanosoma cruzi*: asymmetric responses of bacteria to an infected blood meal. Parasit Vectors. 2016 Dec 9;9(1):636. doi: 10.1186/s13071-016-1926-2.
- Durán P., Siñani E., and Depickère S. (2016). On triatomines, cockroaches and haemolymphagy under laboratory conditions: new discoveries. Mem Inst Oswaldo Cruz. 2016 Oct;111(10):605-613. doi: 10.1590/0074-02760160027.

- Edgar R.C. (2004). MUSCLE: multiple sequence alignment with high accuracy and high throughput. Nucleic Acids Res. 2004 Mar 19;32(5):1792-7. doi: 10.1093/nar/gkh340.
- Eicher, S.C., and Dehio C. (2012). *Bartonella* entry mechanisms into mammalian host cells. Cell Microbiol. 2012 Aug;14(8):1166-73. doi: 10.1111/j.1462-5822.2012.01806.x.
- Eisenberg, E., and Levanon, E.Y. (2013). Human housekeeping genes, revisited. Trends Genet. 2013 Oct;29(10):569-74. doi: 10.1016/j.tig.2013.05.010.
- Fraser, C., Hanage, W.P., and Spratt, B.G. (2007). Recombination and the nature of bacterial speciation. Science. 2007 Jan 26;315(5811):476-80. doi: 10.1126/science.1127573.
- Galan, M., Razzauti, M., Bard, E., Bernard, M., Brouat, C., Charbonnel, N., Dehne-Garcia, A., Loiseau, A., Tatard, C., Tamisier, L., Vayssier-Taussat, M., Vignes, H., & Cosson, J. F. (2016). 16S rRNA Amplicon Sequencing for Epidemiological Surveys of Bacteria in Wildlife. *mSystems*, *1*(4), e00032-16. doi:10.1128/mSystems.00032-16
- Galvão, C., Carcavallo, R., Rocha, D.D.S., and Jurberg, J. (2003). A checklist of the current valid species of the subfamily Triatominae Jeannel, 1919 (Hemiptera, Reduviidae) and their geographical distribution, with nomenclatural and taxonomic notes. *Zootaxa* 202, 1–36. doi: 10.11646/zootaxa.202.1.1
- Garcia M.N., Burroughs H., Gorchakov R., Gunter S.M., Dumonteil E., Murray K.O., and Herrera C.P. (2017). Molecular identification and genotyping of *Trypanosoma cruzi* DNA in autochthonous Chagas disease patients from Texas, USA. Infect Genet Evol. 2017 Apr; 49:151-156. doi: 10.1016/j.meegid.2017.01.016.

- Gilbert, J. A., Meyer, F., Antonopoulos, D., Balaji, P., Brown, C. T., Brown, C. T., Desai, N., Eisen, J. A., Evers, D., Field, D., Feng, W., Huson, D., Jansson, J., Knight, R., Knight, J., Kolker, E., Konstantindis, K., Kostka, J., Kyrpides, N., Mackelprang, R., McHardy A., Quince C., Raes J., Sczyrba A., Shade A., and Stevens, R. (2010). Meeting report: the terabase metagenomics workshop and the vision of an Earth microbiome project. *Standards in genomic sciences*, *3*(3), 243–248. doi:10.4056/sigs.1433550
- Groussin M., Poyet M., Sistiaga A., Kearney S.M., Moniz K., Noel M., Hooker J., Gibbons S.M., Segurel L., Froment A., Mohamed R.S., Fezeu A., Juimo V.A., Lafosse S., Tabe F.E., Girard C., Iqaluk D., Nguyen L.T.T., Shapiro B.J., Lehtimäki J., Ruokolainen L., Kettunen P.P., Vatanen T., Sigwazi S., Mabulla A., Domínguez-Rodrigo M., Nartey Y.A., Agyei-Nkansah A., Duah A., Awuku Y.A., Valles K.A., Asibey S.O., Afihene M.Y., Roberts L.R., Plymoth A., Onyekwere C.A., Summons R.E., Xavier R.J., and Alm E.J. (2021). Elevated rates of horizontal gene transfer in the industrialized human microbiome. Cell. 2021 Apr 15;184(8):2053-2067.e18. doi: 10.1016/j.cell.2021.02.052.
- Guindon S., Dufayard J.F., Lefort V., Anisimova M., Hordijk W., and Gascuel O. (2010). New algorithms and methods to estimate maximum-likelihood phylogenies: assessing the performance of PhyML 3.0. Syst Biol. 2010 May;59(3):307-21. doi: 10.1093/sysbio/syq010. E
- Gutiérrez, R., Krasnov, B., Morick, D., Gottlieb, Y., Khokhlova, I.S., and Harrus, S. (2015). *Bartonella* infection in rodents and their flea ectoparasites: an overview. Vector Borne Zoonotic Dis. 2015 Jan;15(1):27-39. doi: 10.1089/vbz.2014.1606.
- Gürtler R.E., Cecere M.C., Lauricella M.A., Cardinal M.V., Kitron U., and Cohen J.E. (2007) Domestic dogs and cats as sources of *Trypanosoma cruzi* infection in rural northwestern Argentina. Parasitology. 2007 Jan;134(Pt 1):69-82. doi: 10.1017/S0031182006001259.

- Indacochea, A., Gard, C.C., Hansen, I.A., Pierce, J., and Romero, A. (2017). Short-Range Responses of the Kissing Bug *Triatoma rubida* (Hemiptera: Reduviidae) to Carbon Dioxide, Moisture, and Artificial Light. Insects. 2017 Aug 29;8(3):90. doi: 10.3390/insects8030090.
- Jans, C., De Wouters, T., Bonfoh, B., Lacroix, C., Kaindi, D. W. M., Anderegg, J., Böck, D., Vitali, S., Schmid, T., Isenring, J., Kurt, F., Kogi-Makau, W., and Meile, L. (2016). Phylogenetic, epidemiological and functional analyses of the Streptococcus bovis/Streptococcus equinus complex through an overarching MLST scheme. BMC Microbiol. 2016 Jun 21;16(1):117. doi: 10.1186/s12866-016-0735-2.
- Kaiser P.O., Riess, T., O'Rourke, F., Linke, D., and Kempf V.A.J. (2011). *Bartonella spp.:* throwing light on uncommon human infections. Int J Med Microbiol. 2011 Jan;301(1):7-15. doi: 10.1016/j.ijmm.2010.06.004.
- Klepzig, K.D., Adams, A.S., Handelsman, J., and Raffa, K.F. (2009). Symbioses: a key driver of insect physiological processes, ecological interactions, evolutionary diversification, and impacts on humans. Environ Entomol. 2009 Feb;38(1):67-77. doi: 10.1603/022.038.0109.
- Klotz, J.H., Dorn, P.L., Logan, J.L., Stevens, L., Pinnas, J.L., Schmidt, J.O., and Klotz, S.A. (2010). "Kissing bugs": potential disease vectors and cause of anaphylaxis. Clin Infect Dis. 2010 Jun 15;50(12):1629-34. doi: 10.1086/652769.
- Klotz S.A., Dorn P.L., Mosbacher M. and Schmidt J.O. (2014). Kissing bugs in the United States: risk for vector-borne disease in humans. Environ Health Insights. 2014 Dec 10;8(Suppl 2):49-59. doi: 10.4137/EHI.S16003.

- Kloubert, V., and Rink, L. (2019). Selection of an inadequate housekeeping gene leads to misinterpretation of target gene expression in zinc deficiency and zinc supplementation models. J Trace Elem Med Biol. 2019 Dec;56:192-197. doi: 10.1016/j.jtemb.2019.08.007.
- Kosoy, M., McKee, C., Albayrak, L., & Fofanov, Y. (2018). Genotyping of *Bartonella* bacteria and their animal hosts: current status and perspectives. *Parasitology*, *145*(5), 543–562. doi:10.1017/S0031182017001263
- Krasnov, B.R., and Khokhlova, I.S. (2001). The effect of behavioural interactions on the transfer of fleas (Siphonaptera) between two rodent species. J Vector Ecol. 2001 Dec;26(2):181-90. doi:10.1186/S13071020044926
- Krasnov, B.R., Morand, S., Hawlena, H., Khokhlova, I.S., and Shenbrot, G. I. (2005). Sex-biased parasitism, seasonality and sexual size dimorphism in desert rodents. Oecologia. 2005 Dec;146(2):209-17. doi: 10.1007/s00442-005-0189-y.
- La Scola, B., Zeaiter, Z., Khamis, A., and Raoult, D. (2003). Gene-sequence-based criteria for species definition in bacteriology: the *Bartonella* paradigm. Trends Microbiol. 2003 Jul;11(7):318-21. doi: 10.1016/s0966-842x(03)00143-4.
- Lazzari, C.R., Pereira, M.H., and Lorenzo, M.G. (2013). Behavioural biology of Chagas disease vectors. Mem Inst Oswaldo Cruz. 2013;108 Suppl 1(Suppl 1):34-47. doi: 10.1590/0074-0276130409.
- Lloyd-Price, J., Mahurkar, A., Rahnavard, G., Crabtree, J., Orvis, J., Hall, A. B., Brady, A., Creasy, H. H., McCracken, C., Giglio, M. G., McDonald, D., Franzosa, E. A., Knight, R., White, O., and Huttenhower, C. (2017). Strains, functions and dynamics in the expanded Human Microbiome Project. *Nature*, *550*(7674), 61–66. doi:10.1038/nature23889
- Logan, J., Hall, J. L., Chalker, V. J., O'Connell, B., & Birtles, R. J. (2019). *Bartonella clarridgeiae* infection in a patient with aortic root abscess and endocarditis. *Access microbiology*, *1*(10), e000064. doi:10.1099/acmi.0.000064

- Mann, A.E., Mitchell, E.A., Zhang, Y., Curtis-Robles, R., Thapa, S., Hamer, S.A., and Allen, M.S. (2020). Comparison of the Bacterial Gut Microbiome of North American *Triatoma* spp. With and Without *Trypanosoma cruzi*. Front Microbiol. 2020 Mar 13;11:364. doi: 10.3389/fmicb.2020.00364.
- Margos, G., Gatewood, A.G., Aanesen, D.M., Hanincova, K., Terekhova, D., Vollmer, S.A., Conet, M., Piesman, J., Donaghy, M., Bormane, A., Hurn, M.A., Feil, E.J., Fish, D., Casjens, S., Wormser, G.P., Schwartz, I., and Kurtenbach, K. (2008). MLST of housekeeping genes captures geographic population structure and suggests a European origin of Borrelia burgdorferi. Proc Natl Acad Sci U S A. 2008 Jun 24;105(25):8730-5. doi: 10.1073/pnas.0800323105.
- Matsuo Y., Komiya S., Yasumizu Y., Yasuoka Y., Mizushima K., Takagi T., Kryukov K., Fukuda A., Morimoto Y., Naito Y., Okada H., Bono H., Nakagawa S., and Hirota K. (2021). Full-length 16S rRNA gene amplicon analysis of human gut microbiota using MinION™ nanopore sequencing confers species-level resolution. BMC Microbiol. 2021 Jan 26;21(1):35. doi: 10.1186/s12866-021-02094-5.
- McKee C.D., Bai Y., Webb C.T., and Kosoy M.Y. (2021). Bats are key hosts in the radiation of mammal-associated *Bartonella* bacteria. Infect Genet Evol. 2021 Apr;89:104719. doi: 10.1016/j.meegid.2021.104719.
- Mediannikov, O., El Karkouri, K., Diatta, G., Robert, C., Fournier, P. E., and Raoult, D. (2013). Non-contiguous finished genome sequence and description of *Bartonella senegalensis sp*. nov. Stand Genomic Sci. 2013 Jun 6;8(2):279-89. doi: 10.4056/sigs.3807472.

- Nasereddin, A., Risheq, A., Harrus, S., Azmi, K., Ereqat, S., Baneth, G., Salant, H., Mumcuoglu, K.Y., and Abdeen, Z. (2014). *Bartonella* species in fleas from Palestinian territories: prevalence and genetic diversity. J Vector Ecol. 2014 Dec;39(2):261-70. doi: 10.1111/jvec.12100.
- Ogier, J.C., Pagès, S., Galan, M., Barret, M., and Gaudriault, S. (2019). rpoB, a promising marker for analyzing the diversity of bacterial communities by amplicon sequencing. BMC Microbiol. 2019 Jul 29;19(1):171. doi: 10.1186/s12866-019-1546-z.
- Paziewska, A., Harris, P.D., Zwolińska, L., Bajer, A., and Siński, E. (2011). Recombination within and between species of the alpha proteobacterium *Bartonella* infecting rodents. Microb Ecol. 2011 Jan;61(1):134-45. doi: 10.1007/s00248-010-9735-1.
- Pfeiler, E., Bitler, B.G., Ramsey, J.M., Palacios-Cardiel, C., and Markow, T.A. (2006). Genetic variation, population structure, and phylogenetic relationships of *Triatoma rubida* and *T. recurva* (Hemiptera: Reduviidae: Triatominae) from the Sonoran Desert, insect vectors of the Chagas' disease parasite *Trypanosoma cruzi*. Mol Phylogenet Evol. 2006 Oct;41(1):209-21. doi: 10.1016/j.ympev.2006.07.001.
- Poirier, S., Rue, O., Peguilhan, R., Coeuret, G., Zagorec, M., Champomier-Verges M. C., Loux, V., and Chaillou, S. (2018). Deciphering intra-species bacterial diversity of meat and seafood spoilage microbiota using gyrB amplicon sequencing: A comparative analysis with 16S rDNA V3-V4 amplicon sequencing. PLoS One. 2018 Sep 25;13(9):e0204629. doi: 10.1371/journal.pone.0204629.
- Renesto, P., Gouvernet, J., Drancourt, M., Roux, V., and Raoult, D. (2001). Use of rpoB gene analysis for detection and identification of *Bartonella* species. J Clin Microbiol. 2001 Feb;39(2):430-7. doi: 10.1128/JCM.39.2.430-437.2001.

- Ribeiro, J.M.C., Assumpção, T.C.F., Pham, V.M., Francischetti I.M.B., and Reiseman C.E. (2012). An insight into the sialotranscriptome of *Triatoma rubida* (Hemiptera: Heteroptera). J Med Entomol. 2012 May;49(3):563-72. doi: 10.1603/me11243.
- Rodríguez-Ruano, S.M., Škochová, V., Rego, R.O.M., Schmidt, J.O., Roachell, W., Hypša, V., and Nováková, E. (2018). Microbiomes of North American Triatominae: The Grounds for Chagas Disease Epidemiology. Front Microbiol. 2018 Jun 13;9:1167. doi: 10.3389/fmicb.2018.01167.
- *Schulein, R., Seubert, A., Gille, C., Lanz, C., Hansmann, Y., Piémont, Y.,* and Dehio*, C.* (2001). Invasion and persistent intracellular colonization of erythrocytes. A unique parasitic strategy of the emerging pathogen *Bartonella.* J Exp Med. 2001 May 7;193(9):1077-86. doi: 10.1084/jem.193.9.1077.
- Sgro, G. G., Oka, G. U., Souza, D. P., Cenens, W., Bayer-Santos, E., Matsuyama, B. Y., Bueno, N. F., Dos Santos, T. R., Alvarez-Martinez, C. E., Salinas, R. K., & Farah, C. S. (2019). Bacteria-Killing Type IV Secretion Systems. *Frontiers in microbiology*, *10*, 1078. doi:10.3389/fmicb.2019.01078
- Song L., and Xie K. (2020). Engineering CRISPR/Cas9 to mitigate abundant host contamination for 16S rRNA gene-based amplicon sequencing. Microbiome. 2020 Jun 3;8(1):80. doi: 10.1186/s40168-020-00859-0.
- Thellin, O., Zorzi, W., Lakaye B., De Borman, B., Coumans, B., Hennen, G., Grisar, T., Igout, A., and Heinen, E. (1999). Housekeeping genes as internal standards: use and limits. J Biotechnol. 1999 Oct 8;75(2-3):291-5. doi: 10.1016/s0168-1656(99)00163-7.
- Vallejo, G. A., Guhl, F., & Schaub, G. A. (2009). Triatominae-*Trypanosoma cruzi*/*T. rangeli*: Vector-parasite interactions. *Acta tropica*, *110*(2-3), 137–147. doi:10.1016/j.actatropica.2008.10.001

- Vieira, C.B., Praça, Y.R., Bentes, K.L.D.S., Santiago, P.B., Silva, S.M.M., Silva, G.D.S., Motta, F.N., Bastos, I.M.D., Santana, J.M., and De Araújo, C. N. (2018). Triatomines: Trypanosomatids, Bacteria, and Viruses Potential Vectors? Front Cell Infect Microbiol. 2018 Nov 16;8:405. doi: 10.3389/fcimb.2018.00405.
- Waltmann, A., Willcox, A.C., Balasubramanian, S., Borrini Mayori K., Mendoza Guerrero, S., Salazar Sanchez, R.S., Roach, J., Condori Pino, C., Gilman, R.H., Bern, C., Juliano, J.J., Levy, M.Z., Meshnick, S.R., and Bowman, N.M. (2019). Hindgut microbiota in laboratory-reared and wild *Triatoma* infestans. PLoS Negl Trop Dis. 2019 May 6;13(5):e0007383. doi: 10.1371/journal.pntd.0007383.

8. Appendix

Table 9: Year of collection, sample name, location, coordinates and larval stage of the samples used for PCR screening targeting towards *Bartonella*

Year of collection	Sample name	Location	Coordinates	Larval Stage
2018	LC1i1A2	Las Cienegas National Conservation Area	31° 46′ 48″ N, 110° 37′ 08″ W	1
2018	LC1i1B2	Las Cienegas National Conservation Area	31° 46′ 48″ N, 110° 37′ 08″ W	1
2018	LC1i1C0	Las Cienegas National Conservation Area	31° 46′ 48″ N, 110° 37′ 08″ W	1
2018	LC1i1D0	Las Cienegas National Conservation Area	31° 46′ 48″ N, 110° 37′ 08″ W	1
2018	LC2i2A2	Las Cienegas National Conservation Area	31° 46′ 48″ N, 110° 37′ 08″ W	2
2018	LC2i2C2	Las Cienegas National Conservation Area	31° 46′ 48″ N, 110° 37′ 08″ W	2

2018	LC2i2D2	Las Cienegas National Conservation Area	31° 46′ 48″ N, 110° 37′ 08″ W	2
2018	LC2i2E1	Las Cienegas National Conservation Area	31° 46′ 48″ N, 110° 37′ 08″ W	2
2018	LC3i3B2	Las Cienegas National Conservation Area	31° 46′ 48″ N, 110° 37′ 08″ W	3
2018	LC4i1A0	Las Cienegas National Conservation Area	31° 46′ 48″ N, 110° 37′ 08″ W	1
2018	LC4i1B0	Las Cienegas National Conservation Area	31° 46′ 48″ N, 110° 37′ 08″ W	1
2018	LC4i1C0	Las Cienegas National Conservation Area	31° 46′ 48″ N, 110° 37′ 08″ W	1
2018	LC5i1A3	Las Cienegas National Conservation Area	31° 46′ 48″ N, 110° 37′ 08″ W	1
2018	LC5i1B3	Las Cienegas National Conservation Area	31° 46′ 48″ N, 110° 37′ 08″ W	1
2018	LC5i1D3	Las Cienegas National Conservation Area	31° 46′ 48″ N, 110° 37′ 08″ W	1
2018	LC7i2A2	Las Cienegas National Conservation Area	31° 46′ 48″ N, 110° 37′ 08″ W	2
2018	LC7i2B2	Las Cienegas National Conservation Area	31° 46′ 48″ N, 110° 37′ 08″ W	2
2018	LC7i2C2	Las Cienegas National Conservation Area	31° 46′ 48″ N, 110° 37′ 08″ W	2
2018	LC10i1A1	Las Cienegas National Conservation Area	31° 46′ 48″ N, 110° 37′ 08″ W	1
2018	LC10i1B1	Las Cienegas National Conservation Area	31° 46′ 48″ N, 110° 37′ 08″ W	1
2018	LC10i1C1	Las Cienegas National Conservation Area	31° 46′ 48″ N, 110° 37′ 08″ W	1

2018	LC10i1D1	Las Cienegas National Conservation Area	31° 46′ 48″ N, 110° 37′ 08″ W	1
2018	LC10i1E1	Las Cienegas National Conservation Area	31° 46′ 48″ N, 110° 37′ 08″ W	1
2018	LC11i2A1	Las Cienegas National Conservation Area	31° 46′ 48″ N, 110° 37′ 08″ W	2
2018	LC11i2B1	Las Cienegas National Conservation Area	31° 46′ 48″ N, 110° 37′ 08″ W	2
2018	LC11i2C1	Las Cienegas National Conservation Area	31° 46′ 48″ N, 110° 37′ 08″ W	2
2018	LC11i2D1	Las Cienegas National Conservation Area	31° 46′ 48″ N, 110° 37′ 08″ W	2
2018	LC13i3A3	Las Cienegas National Conservation Area	31° 46′ 48″ N, 110° 37′ 08″ W	3
2018	LC13i3B3	Las Cienegas National Conservation Area	31° 46′ 48″ N, 110° 37′ 08″ W	3
2018	LC14i4A2	Las Cienegas National Conservation Area	31° 46′ 48″ N, 110° 37′ 08″ W	4
2018	LC14i4B1	Las Cienegas National Conservation Area	31° 46′ 48″ N, 110° 37′ 08″ W	4
2018	LC28i2A1	Las Cienegas National Conservation Area	31° 46′ 48″ N, 110° 37′ 08″ W	2
2018	LC28i2B2	Las Cienegas National Conservation Area	31° 46′ 48″ N, 110° 37′ 08″ W	2
2018	LC28i2C2	Las Cienegas National Conservation Area	31° 46′ 48″ N, 110° 37′ 08″ W	2
2018	LC33i2A3	Las Cienegas National Conservation Area	31° 46′ 48″ N, 110° 37′ 08″ W	2
2018	LC33i2B3	Las Cienegas National Conservation Area	31° 46′ 48″ N, 110° 37′ 08″ W	2

2018	LC33i2C3	Las Cienegas National Conservation Area	31° 46′ 48″ N, 110° 37′ 08″ W	2
2018	TU2i4A3	University of Arizona Desert Station	32° 14' 55.7304" N, 110° 59' 14.7084" W	4
2018	TU2i4B3	University of Arizona Desert Station	32° 14' 55.7304" N, 110° 59' 14.7084" W	4
2018	TU3i4A3	University of Arizona Desert Station	32° 14' 55.7304" N, 110° 59' 14.7084" W	4
2018	TU3i4B3	University of Arizona Desert Station	32° 14' 55.7304" N, 110° 59' 14.7084" W	4
2018	TU30i3A3	University of Arizona Desert Station	32° 14' 55.7304" N, 110° 59' 14.7084" W	3
2018	TU30i3B3	University of Arizona Desert Station	32° 14' 55.7304" N, 110° 59' 14.7084" W	3
2018	TU30i3C3	University of Arizona Desert Station	32° 14' 55.7304" N, 110° 59' 14.7084" W	3
2018	TU30i3D3	University of Arizona Desert Station	32° 14' 55.7304" N, 110° 59' 14.7084" W	3
2018	TU30i3E3	University of Arizona Desert Station	32° 14' 55.7304" N, 110° 59' 14.7084" W	3
2018	TU30i3F3	University of Arizona Desert Station	32° 14' 55.7304" N, 110° 59' 14.7084" W	3
2018	TU36i4A3	University of Arizona Desert Station	32° 14' 55.7304" N, 110° 59' 14.7084" W	4
2018	TU36i4B3	University of Arizona Desert Station	32° 14' 55.7304" N, 110° 59' 14.7084" W	4
2018	TU36i4C3	University of Arizona Desert Station	32° 14' 55.7304" N, 110° 59' 14.7084" W	4
2018	TU37i4A3	University of Arizona Desert Station	32° 14' 55.7304" N, 110° 59' 14.7084" W	4

2018	TU37i4B3	University of Arizona Desert Station	32° 14' 55.7304" N, 110° 59' 14.7084" W	4
2018	TU37i4C3	University of Arizona Desert Station	32° 14' 55.7304" N, 110° 59' 14.7084" W	4
2018	TU39i4A1	University of Arizona Desert Station	32° 14' 55.7304" N, 110° 59' 14.7084" W	4
2018	TU39i4B1	University of Arizona Desert Station	32° 14' 55.7304" N, 110° 59' 14.7084" W	4
2018	TU39i4C1	University of Arizona Desert Station	32° 14' 55.7304" N, 110° 59' 14.7084" W	4
2018	TU40i3A3	University of Arizona Desert Station	32° 14' 55.7304" N, 110° 59' 14.7084" W	3
2018	TU40i3B3	University of Arizona Desert Station	32° 14' 55.7304" N, 110° 59' 14.7084" W	3
2018	TU41i3A2	University of Arizona Desert Station	32° 14' 55.7304" N, 110° 59' 14.7084" W	3
2018	TU41i3B2	University of Arizona Desert Station	32° 14' 55.7304" N, 110° 59' 14.7084" W	3
2018	TU50i3B3	University of Arizona Desert Station	32° 14' 55.7304" N, 110° 59' 14.7084" W	3
2018	TU54i4A3	University of Arizona Desert Station	32° 14' 55.7304" N, 110° 59' 14.7084" W	4
2018	TU54i4B2	University of Arizona Desert Station	32° 14' 55.7304" N, 110° 59' 14.7084" W	4
2018	TU55i4A1	University of Arizona Desert Station	32° 14' 55.7304" N, 110° 59' 14.7084" W	4
2018	TU55i4B1	University of Arizona Desert Station	32° 14' 55.7304" N, 110° 59' 14.7084" W	4
2018	TU55i4C1	University of Arizona Desert Station	32° 14' 55.7304" N, 110° 59' 14.7084" W	4

2018	TU55i4D1	University of Arizona Desert Station	32° 14' 55.7304" N, 110° 59' 14.7084" W	4
2018	TU56i3A3	University of Arizona Desert Station	32° 14' 55.7304" N, 110° 59' 14.7084" W	3
2018	TU56i3C3	University of Arizona Desert Station	32° 14' 55.7304" N, 110° 59' 14.7084" W	3
2018	TU57i3A1	University of Arizona Desert Station	32° 14' 55.7304" N, 110° 59' 14.7084" W	3
2018	TU57i3B1	University of Arizona Desert Station	32° 14' 55.7304" N, 110° 59' 14.7084" W	3
2018	TU57i3C1	University of Arizona Desert Station	32° 14' 55.7304" N, 110° 59' 14.7084" W	3
2018	TU57i3D1	University of Arizona Desert Station	32° 14' 55.7304" N, 110° 59' 14.7084" W	3
2018	TU60i2A3	University of Arizona Desert Station	32° 14' 55.7304" N, 110° 59' 14.7084" W	2
2018	TU60i2B3	University of Arizona Desert Station	32° 14' 55.7304" N, 110° 59' 14.7084" W	2
2018	TU60i2C3	University of Arizona Desert Station	32° 14' 55.7304" N, 110° 59' 14.7084" W	2
2018	TU60i2D2	University of Arizona Desert Station	32° 14' 55.7304" N, 110° 59' 14.7084" W	2
2018	TU68i2A2	University of Arizona Desert Station	32° 14' 55.7304" N, 110° 59' 14.7084" W	2
2018	TU68i2B2	University of Arizona Desert Station	32° 14' 55.7304" N, 110° 59' 14.7084" W	2
2018	TU68i2C2	University of Arizona Desert Station	32° 14' 55.7304" N, 110° 59' 14.7084" W	2
2018	TU68i2D2	University of Arizona Desert Station	32° 14' 55.7304" N, 110° 59' 14.7084" W	2

2018	TU1i4A3	University of Arizona Desert Station	32° 14' 55.7304" N, 110° 59' 14.7084" W	4
2018	TU4i3A3	University of Arizona Desert Station	32° 14' 55.7304" N, 110° 59' 14.7084" W	3
2018	TU5i4A1	University of Arizona Desert Station	32° 14' 55.7304" N, 110° 59' 14.7084" W	4
2018	TU7i6A0	University of Arizona Desert Station	32° 14' 55.7304" N, 110° 59' 14.7084" W	6
2018	TU8i6A0	University of Arizona Desert Station	32° 14' 55.7304" N, 110° 59' 14.7084" W	6
2018	TU9i6A0	University of Arizona Desert Station	32° 14' 55.7304" N, 110° 59' 14.7084" W	6
2018	TU10i6A0	University of Arizona Desert Station	32° 14' 55.7304" N, 110° 59' 14.7084" W	6
2018	TU11i6A0	University of Arizona Desert Station	32° 14' 55.7304" N, 110° 59' 14.7084" W	6
2018	TU12i6A0	University of Arizona Desert Station	32° 14' 55.7304" N, 110° 59' 14.7084" W	6
2018	TU13i6A2	University of Arizona Desert Station	32° 14' 55.7304" N, 110° 59' 14.7084" W	6
2018	TU14i6A0	University of Arizona Desert Station	32° 14' 55.7304" N, 110° 59' 14.7084" W	6
2018	TU15i6A0	University of Arizona Desert Station	32° 14' 55.7304" N, 110° 59' 14.7084" W	6
2018	TU16i6A0	University of Arizona Desert Station	32° 14' 55.7304" N, 110° 59' 14.7084" W	6
2018	TU17i6A0	University of Arizona Desert Station	32° 14' 55.7304" N, 110° 59' 14.7084" W	6
2018	TU18i6A0	University of Arizona Desert Station	32° 14' 55.7304" N, 110° 59' 14.7084" W	6

2018	TU19i6A2	University of Arizona Desert Station	32° 14' 55.7304" N, 110° 59' 14.7084" W	6
2018	TU21i6A1	University of Arizona Desert Station	32° 14' 55.7304" N, 110° 59' 14.7084" W	6
2018	TU22i6A1	University of Arizona Desert Station	32° 14' 55.7304" N, 110° 59' 14.7084" W	6
2018	TU24i5A1	University of Arizona Desert Station	32° 14' 55.7304" N, 110° 59' 14.7084" W	5
2018	TU25i5A3	University of Arizona Desert Station	32° 14' 55.7304" N, 110° 59' 14.7084" W	5
2018	TU38i4A2	University of Arizona Desert Station	32° 14' 55.7304" N, 110° 59' 14.7084" W	4
2018	TU42i3A1	University of Arizona Desert Station	32° 14' 55.7304" N, 110° 59' 14.7084" W	3
2018	TU44i6A3	University of Arizona Desert Station	32° 14' 55.7304" N, 110° 59' 14.7084" W	6
2018	TU45i4A1	University of Arizona Desert Station	32° 14' 55.7304" N, 110° 59' 14.7084" W	4
2018	TU46i6A0	University of Arizona Desert Station	32° 14' 55.7304" N, 110° 59' 14.7084" W	6
2018	TU47i4A3	University of Arizona Desert Station	32° 14' 55.7304" N, 110° 59' 14.7084" W	4
2018	TU48i4A1	University of Arizona Desert Station	32° 14' 55.7304" N, 110° 59' 14.7084" W	4
2018	TU51i2A2	University of Arizona Desert Station	32° 14' 55.7304" N, 110° 59' 14.7084" W	2
2018	TU63i6A1	University of Arizona Desert Station	32° 14' 55.7304" N, 110° 59' 14.7084" W	6
2018	TU64i4A2	University of Arizona Desert Station	32° 14' 55.7304" N, 110° 59' 14.7084" W	4

2018	TU65i3A2	University of Arizona Desert Station	32° 14' 55.7304" N, 110° 59' 14.7084" W	3
2018	TU67i3A2	University of Arizona Desert Station	32° 14' 55.7304" N, 110° 59' 14.7084" W	3
2018	TU73i3A0	University of Arizona Desert Station	32° 14' 55.7304" N, 110° 59' 14.7084" W	3
2018	TU74i4A1	University of Arizona Desert Station	32° 14' 55.7304" N, 110° 59' 14.7084" W	4
2018	LC12i2A2	Las Cienegas National Conservation Area	31° 46′ 48″ N, 110° 37′ 08″ W	2
2018	LC15i5A3	Las Cienegas National Conservation Area	31° 46′ 48″ N, 110° 37′ 08″ W	5
2018	LC16i5A1	Las Cienegas National Conservation Area	31° 46′ 48″ N, 110° 37′ 08″ W	5
2018	LC17i6A1	Las Cienegas National Conservation Area	31° 46′ 48″ N, 110° 37′ 08″ W	6
2018	LC18i6A2	Las Cienegas National Conservation Area	31° 46′ 48″ N, 110° 37′ 08″ W	6
2018	LC26i6A1	Las Cienegas National Conservation Area	31° 46′ 48″ N, 110° 37′ 08″ W	6
2018	LC32i5A1	Las Cienegas National Conservation Area	31° 46′ 48″ N, 110° 37′ 08″ W	5
2018	LC37i1A3	Las Cienegas National Conservation Area	31° 46′ 48″ N, 110° 37′ 08″ W	1
2019	DS16I6M	University of Arizona Desert Station	32° 14' 55.7304" N, 110° 59' 14.7084" W	6
2019	DS16I6F	University of Arizona Desert Station	32° 14' 55.7304" N, 110° 59' 14.7084" W	6
2019	DS3I3A	University of Arizona Desert Station	32° 14' 55.7304" N, 110° 59' 14.7084" W	3

2019	DS3I3B	University of Arizona Desert Station	32° 14' 55.7304" N, 110° 59' 14.7084" W	3
2019	DS3I3C	University of Arizona Desert Station	32° 14' 55.7304" N, 110° 59' 14.7084" W	3
2019	DS16I2A	University of Arizona Desert Station	32° 14' 55.7304" N, 110° 59' 14.7084" W	2
2019	DS16I2B	University of Arizona Desert Station	32° 14' 55.7304" N, 110° 59' 14.7084" W	2
2019	DS16I2C	University of Arizona Desert Station	32° 14' 55.7304" N, 110° 59' 14.7084" W	2
2019	DS16I2D	University of Arizona Desert Station	32° 14' 55.7304" N, 110° 59' 14.7084" W	2
2019	DS3I5A	University of Arizona Desert Station	32° 14' 55.7304" N, 110° 59' 14.7084" W	5
2019	DS3I5B	University of Arizona Desert Station	32° 14' 55.7304" N, 110° 59' 14.7084" W	5
2019	DS3I6A	University of Arizona Desert Station	32° 14' 55.7304" N, 110° 59' 14.7084" W	6
2019	DS3I6B	University of Arizona Desert Station	32° 14' 55.7304" N, 110° 59' 14.7084" W	6
2019	DS16I1A	University of Arizona Desert Station	32° 14' 55.7304" N, 110° 59' 14.7084" W	1
2019	DS16I1B	University of Arizona Desert Station	32° 14' 55.7304" N, 110° 59' 14.7084" W	1
2019	DS16I1D	University of Arizona Desert Station	32° 14' 55.7304" N, 110° 59' 14.7084" W	1
2019	DS16I1E	University of Arizona Desert Station	32° 14' 55.7304" N, 110° 59' 14.7084" W	1
2019	DS16I1F	University of Arizona Desert Station	32° 14' 55.7304" N, 110° 59' 14.7084" W	1

2019	DS16I5A	University of Arizona Desert Station	32° 14' 55.7304" N, 110° 59' 14.7084" W	5
2019	DS3I5	University of Arizona Desert Station	32° 14' 55.7304" N, 110° 59' 14.7084" W	5
2019	DS3I6	University of Arizona Desert Station	32° 14' 55.7304" N, 110° 59' 14.7084" W	6
2019	DS13I6	University of Arizona Desert Station	32° 14' 55.7304" N, 110° 59' 14.7084" W	6
2019	DS5I6A	University of Arizona Desert Station	32° 14' 55.7304" N, 110° 59' 14.7084" W	6
2019	DS5I6B	University of Arizona Desert Station	32° 14' 55.7304" N, 110° 59' 14.7084" W	6
2019	DS12I6M	University of Arizona Desert Station	32° 14' 55.7304" N, 110° 59' 14.7084" W	6
2019	DS18I6	University of Arizona Desert Station	32° 14' 55.7304" N, 110° 59' 14.7084" W	6
2019	DS12I6F	University of Arizona Desert Station	32° 14' 55.7304" N, 110° 59' 14.7084" W	6
2019	DS15I6	University of Arizona Desert Station	32° 14' 55.7304" N, 110° 59' 14.7084" W	6
2019	DS6I6	University of Arizona Desert Station	32° 14' 55.7304" N, 110° 59' 14.7084" W	6
2019	DS5I6	University of Arizona Desert Station	32° 14' 55.7304" N, 110° 59' 14.7084" W	6
2019	DS3M-A	University of Arizona Desert Station	32° 14' 55.7304" N, 110° 59' 14.7084" W	-

Table 10: Year of collection, sample name, location and coordinates of the samples used for *Bartonella* amplicon sequencing

Year of collection	**Sample name**	**Location**	**Geographic origin**
2018	TU81i5A0	University of Arizona Desert Station	32° 14' 55.7304" N, 110° 59' 14.7084" W
2018	TU79i5A3	University of Arizona Desert Station	32° 14' 55.7304" N, 110° 59' 14.7084" W
2018	TU74i4A1	University of Arizona Desert Station	32° 14' 55.7304" N, 110° 59' 14.7084" W
2018	TU71i5A1	University of Arizona Desert Station	32° 14' 55.7304" N, 110° 59' 14.7084" W
2018	TU69i6A1	University of Arizona Desert Station	32° 14' 55.7304" N, 110° 59' 14.7084" W
2018	TU68i2D2	University of Arizona Desert Station	32° 14' 55.7304" N, 110° 59' 14.7084" W
2018	TU62i3A2	University of Arizona Desert Station	32° 14' 55.7304" N, 110° 59' 14.7084" W
2018	TU60i2D2	University of Arizona Desert Station	32° 14' 55.7304" N, 110° 59' 14.7084" W
2018	TU60i2C3	University of Arizona Desert Station	32° 14' 55.7304" N, 110° 59' 14.7084" W
2018	TU60i2A3	University of Arizona Desert Station	32° 14' 55.7304" N, 110° 59' 14.7084" W
2018	TU59i3A3	University of Arizona Desert Station	32° 14' 55.7304" N, 110° 59' 14.7084" W
2018	TU58i3A1	University of Arizona Desert Station	32° 14' 55.7304" N, 110° 59' 14.7084" W
2018	TU57i3B1	University of Arizona Desert Station	32° 14' 55.7304" N, 110° 59' 14.7084" W

2018	TU57i3A1	University of Arizona Desert Station	32° 14' 55.7304" N, 110° 59' 14.7084" W
2018	TU56i3C3	University of Arizona Desert Station	32° 14' 55.7304" N, 110° 59' 14.7084" W
2018	TU55i4D1	University of Arizona Desert Station	32° 14' 55.7304" N, 110° 59' 14.7084" W
2018	TU55i4C1	University of Arizona Desert Station	32° 14' 55.7304" N, 110° 59' 14.7084" W
2018	TU55i4B1	University of Arizona Desert Station	32° 14' 55.7304" N, 110° 59' 14.7084" W
2018	TU55i4A1	University of Arizona Desert Station	32° 14' 55.7304" N, 110° 59' 14.7084" W
2018	TU54i4B2	University of Arizona Desert Station	32° 14' 55.7304" N, 110° 59' 14.7084" W
2018	TU4i3A3	University of Arizona Desert Station	32° 14' 55.7304" N, 110° 59' 14.7084" W
2018	TU46i6A0	University of Arizona Desert Station	32° 14' 55.7304" N, 110° 59' 14.7084" W
2018	TU45i4A1	University of Arizona Desert Station	32° 14' 55.7304" N, 110° 59' 14.7084" W
2018	TU41i3B2	University of Arizona Desert Station	32° 14' 55.7304" N, 110° 59' 14.7084" W
2018	TU40i3A3	University of Arizona Desert Station	32° 14' 55.7304" N, 110° 59' 14.7084" W
2018	TU3i4B3	University of Arizona Desert Station	32° 14' 55.7304" N, 110° 59' 14.7084" W
2018	TU3i4A3	University of Arizona Desert Station	32° 14' 55.7304" N, 110° 59' 14.7084" W
2018	TU36i4B3	University of Arizona Desert Station	32° 14' 55.7304" N, 110° 59' 14.7084" W

2018	TU30i3F3	University of Arizona Desert Station	32° 14' 55.7304" N, 110° 59' 14.7084" W
2018	TU30i3E3	University of Arizona Desert Station	32° 14' 55.7304" N, 110° 59' 14.7084" W
2018	TU30i3D3	University of Arizona Desert Station	32° 14' 55.7304" N, 110° 59' 14.7084" W
2018	TU30i3C3	University of Arizona Desert Station	32° 14' 55.7304" N, 110° 59' 14.7084" W
2018	TU30i3B3	University of Arizona Desert Station	32° 14' 55.7304" N, 110° 59' 14.7084" W
2018	TU30i3A3	University of Arizona Desert Station	32° 14' 55.7304" N, 110° 59' 14.7084" W
2018	TU2i4A3	University of Arizona Desert Station	32° 14' 55.7304" N, 110° 59' 14.7084" W
2018	TU27i5A0	University of Arizona Desert Station	32° 14' 55.7304" N, 110° 59' 14.7084" W
2018	TU26i5A3	University of Arizona Desert Station	32° 14' 55.7304" N, 110° 59' 14.7084" W
2018	TU25i5A3	University of Arizona Desert Station	32° 14' 55.7304" N, 110° 59' 14.7084" W
2018	TU24i5A1	University of Arizona Desert Station	32° 14' 55.7304" N, 110° 59' 14.7084" W
2018	LC7i2C2	Las Cienegas Conservation Area	31° 46′ 48″ N, 110° 37′ 08″ W
2018	LC7i2B2	Las Cienegas Conservation Area	31° 46′ 48″ N, 110° 37′ 08″ W
2018	LC7i2A2	Las Cienegas Conservation Area	31° 46′ 48″ N, 110° 37′ 08″ W
2018	LC5i1D3	Las Cienegas Conservation Area	31° 46′ 48″ N, 110° 37′ 08″ W

2018	LC4i1A0	Las Cienegas Conservation Area	31° 46′ 48″ N, 110° 37′ 08″ W
2018	LC3i3D2	Las Cienegas Conservation Area	31° 46′ 48″ N, 110° 37′ 08″ W
2018	LC3i3C2	Las Cienegas Conservation Area	31° 46′ 48″ N, 110° 37′ 08″ W
2018	LC3i3B2	Las Cienegas Conservation Area	31° 46′ 48″ N, 110° 37′ 08″ W
2018	LC3i3A2	Las Cienegas Conservation Area	31° 46′ 48″ N, 110° 37′ 08″ W
2018	LC37i1A3	Las Cienegas Conservation Area	31° 46′ 48″ N, 110° 37′ 08″ W
2018	LC33i2B3	Las Cienegas Conservation Area	31° 46′ 48″ N, 110° 37′ 08″ W
2018	LC2i2E1	Las Cienegas Conservation Area	31° 46′ 48″ N, 110° 37′ 08″ W
2018	LC2i2D2	Las Cienegas Conservation Area	31° 46′ 48″ N, 110° 37′ 08″ W
2018	LC2i2C2	Las Cienegas Conservation Area	31° 46′ 48″ N, 110° 37′ 08″ W
2018	LC2i2B2	Las Cienegas Conservation Area	31° 46′ 48″ N, 110° 37′ 08″ W
2018	LC2i2A2	Las Cienegas Conservation Area	31° 46′ 48″ N, 110° 37′ 08″ W
2018	LC28i2C2	Las Cienegas Conservation Area	31° 46′ 48″ N, 110° 37′ 08″ W
2018	LC28i2B2	Las Cienegas Conservation Area	31° 46′ 48″ N, 110° 37′ 08″ W
2018	LC28i2A1	Las Cienegas Conservation Area	31° 46′ 48″ N, 110° 37′ 08″ W

2018	LC25i5A1	Las Cienegas Conservation Area	31° 46′ 48″ N, 110° 37′ 08″ W
2018	LC24i5A3	Las Cienegas Conservation Area	31° 46′ 48″ N, 110° 37′ 08″ W
2018	LC23i4A3	Las Cienegas Conservation Area	31° 46′ 48″ N, 110° 37′ 08″ W
2018	LC21i6A1	Las Cienegas Conservation Area	31° 46′ 48″ N, 110° 37′ 08″ W
2018	LC20i6A0	Las Cienegas Conservation Area	31° 46′ 48″ N, 110° 37′ 08″ W
2018	LC1i1D0	Las Cienegas Conservation Area	31° 46′ 48″ N, 110° 37′ 08″ W
2018	LC1i1C0	Las Cienegas Conservation Area	31° 46′ 48″ N, 110° 37′ 08″ W
2018	LC19i6A0	Las Cienegas Conservation Area	31° 46′ 48″ N, 110° 37′ 08″ W
2018	LC18i6A2	Las Cienegas Conservation Area	31° 46′ 48″ N, 110° 37′ 08″ W
2018	LC14i4B1	Las Cienegas Conservation Area	31° 46′ 48″ N, 110° 37′ 08″ W
2018	LC14i4A2	Las Cienegas Conservation Area	31° 46′ 48″ N, 110° 37′ 08″ W
2018	LC13i3B3	Las Cienegas Conservation Area	31° 46′ 48″ N, 110° 37′ 08″ W
2018	LC11i2D1	Las Cienegas Conservation Area	31° 46′ 48″ N, 110° 37′ 08″ W
2018	LC11i2C1	Las Cienegas Conservation Area	31° 46′ 48″ N, 110° 37′ 08″ W
2018	LC11i2A1	Las Cienegas Conservation Area	31° 46′ 48″ N, 110° 37′ 08″ W

9. Illustration Directory